



# A record of the $\delta^{44/40}\text{Ca}$ and [Sr] of seawater over the last 100 million years from fossil elasmobranch tooth enamel

Alliya A. Akhtar<sup>a,\*</sup>, Lauren M. Santi<sup>b,d</sup>, Michael L. Griffiths<sup>c</sup>, Martin Becker<sup>c</sup>, Robert A. Eagle<sup>b,d</sup>, Sora Kim<sup>e</sup>, László Kocsis<sup>f</sup>, Yair Rosenthal<sup>g</sup>, John A. Higgins<sup>a</sup>

<sup>a</sup> Department of Geosciences, Princeton University, Princeton, NJ, United States of America

<sup>b</sup> Institute of Environment and Sustainability, University of California – Los Angeles, CA, United States of America

<sup>c</sup> William Paterson University, Wayne, NJ, United States of America

<sup>d</sup> Atmospheric and Oceanic Sciences Department, Ecology and Evolutionary Biology Department, University of California – Los Angeles, CA, United States of America

<sup>e</sup> University of California Merced, Department of Life and Environmental Sciences, Merced, CA, United States of America

<sup>f</sup> Geology Group, Faculty of Science, Universiti Brunei Darussalam, Brunei Darussalam

<sup>g</sup> Department of Marine and Coastal Sciences, Rutgers University, New Brunswick, NJ, United States of America

## ARTICLE INFO

### Article history:

Received 25 November 2019

Received in revised form 7 May 2020

Accepted 18 May 2020

Available online 5 June 2020

Editor: L. Derry

### Keywords:

calcium isotopes

Sr/Ca

elasmobranch teeth

marine calcium cycle

seawater chemistry

## ABSTRACT

The global geochemical cycles of calcium and strontium in seawater link the chemical composition of the oceans to the global carbon cycle and Earth's climate through the precipitation, diagenetic alteration, and sedimentary recycling of marine carbonate minerals. Here we present a record of calcium isotopic composition and [Sr] of seawater over the last 100 million years using measurements from modern and fossil shark teeth. Although there is significant variability in modern elasmobranch tooth enamel associated with physiology and diet, our record suggests a first-order increase in the average calcium isotopic composition of seawater by 0.5‰ and a decline in Sr/Ca ratios of ~40% over the last 100 million years. These observations are in agreement with trends seen in other archives. We propose that the observed changes in both the calcium isotopic composition and Sr concentration of seawater can be explained by changes in the partitioning of the global carbonate sink associated with the development of a deep-sea carbonate reservoir in the mid-Mesozoic.

© 2020 Elsevier B.V. All rights reserved.

## 1. Introduction

The isotopic composition of calcium in seawater ( $^{44}\text{Ca}/^{40}\text{Ca}$  or  $\delta^{44/40}\text{Ca}_{\text{sw}}$  in  $\delta$  notation) is enriched in  $^{44}\text{Ca}$  compared to sources (i.e., rivers, groundwater, and high-temperature hydrothermal systems) by ~1‰. This difference is attributed to Ca isotope fractionation associated with the precipitation and burial of marine carbonate minerals. Both laboratory and natural studies indicate that fractionation of Ca isotopes in marine carbonates depends on mineralogy (e.g., calcite vs. aragonite; Gussone et al., 2005) and precipitation rate (Fantle and DePaolo, 2007; Tang et al., 2008; DePaolo, 2011; Nielsen et al., 2013). Studies of Ca isotope mass balance in seawater on geologic timescales have largely focused on the role of carbonate mineralogy, as there is independent geologic evidence for secular changes in the dominant mineralogy of carbonate sediments over the Phanerozoic – the calcite and arago-

nite seas of Sandberg (1983). However, recent studies by Fantle and Higgins (2014) and Higgins et al. (2018) have shown that isotopic effects associated with precipitation rate, in the form of recrystallization/neomorphism during early marine diagenesis in carbonate sediments, can shift bulk sediment  $\delta^{44/40}\text{Ca}$  values by >1‰. According to this model, seawater-buffered diagenetic alteration results in shallow-water carbonate sediments that are enriched in  $^{44}\text{Ca}$  compared to deep-sea carbonate sediments resulting in  $\delta^{44/40}\text{Ca}$  value of the global carbonate sink that is the weighted average of shallow-water and deep-sea carbonate sedimentation (Higgins et al., 2018).

The concentration of Sr in seawater ( $[\text{Sr}]_{\text{sw}}$ ) also depends on the mineralogy and the extent of diagenetic alteration of the global carbonate sediment sink. For example, aragonite precipitated from modern seawater is characterized by Sr contents of ~10 mmol/mol, whereas high-Mg calcite and biogenic low-Mg calcites are associated with somewhat lower Sr contents of (3.8 mmol/mol to 1.2 mmol/mol, respectively; Lear et al., 2003; Higgins et al., 2018). Diagenetic alteration of any of these primary carbonate minerals to calcite and/or dolomite is typically associ-

\* Corresponding author.

E-mail address: aakhtar@princeton.edu (A.A. Akhtar).

ated with a large reduction in Sr content, the magnitude of which depends on whether the alteration occurs under sediment-buffered or fluid-buffered conditions. For example, dolomites interpreted to have formed under seawater-buffered diagenetic conditions are characterized by Sr contents that approach  $\sim 0.1$  mmol/mol (Vahrenkamp and Swart, 1990; Swart and Melim, 2003; Higgins et al., 2018), whereas dolomites that form under sediment-buffered conditions may retain a significant fraction of Sr from the precursor mineral (Ahm et al., 2018; Higgins et al., 2018). A corollary of the behavior of Sr in carbonate minerals during diagenesis is that changes in either the amount and/or style of diagenetic alteration associated with the burial of marine carbonate sediments globally should be associated with changes in  $[\text{Sr}]_{\text{sw}}$ . In particular, widespread seawater-buffered diagenetic alteration of marine carbonate sediments favor elevated seawater  $[\text{Sr}]_{\text{sw}}$  whereas the burial of marine carbonates in environments where they undergo diagenesis under sediment-buffered conditions favors low  $[\text{Sr}]_{\text{sw}}$ .

Reconstructions of seawater  $\delta^{44/40}\text{Ca}$  values and Sr concentrations from fossil corals (Gothmann et al., 2015, 2016), barite (Griffith et al., 2008), brachiopods (Farkaš et al., 2007), benthic foraminifera (Heuser et al., 2005; Sime et al., 2007), phosphates (Soudry et al., 2004, 2006) and bulk carbonates (Fantle and DePaolo, 2005, 2007; Gothmann et al., 2016) show a range of secular variability over the last 100 million years. In general, while all the records indicate an increase in the  $\delta^{44/40}\text{Ca}$  of seawater over the last 25 million years, older records diverge (for example, phosphates suggest a depleted Cretaceous ocean compared to bulk carbonates and brachiopods). Furthermore, the variability in  $\delta^{44/40}\text{Ca}$  observed in some individual archives, such as corals, over the last 100 Ma is larger (approaching 1‰) than the range in others. Additionally, temporal gaps in individual records (e.g. brachiopods) and shorter time ranges (e.g. barite), limit the robustness of seawater reconstructions based on these archives. A multi-archival approach, therefore, allows for a robust understanding of variations and trends in the seawater record. Reconstructions of seawater Sr/Ca exhibit better agreement between archives and indicate constant or slightly declining ratios since the Mesozoic, with the notable exception of records from calcium calcite veins in altered oceanic crust (Coggon et al., 2010; Rausch et al., 2013).

Fossil elasmobranch (shark) teeth represent an archive extensively used to reconstruct ancient seawater chemistry, including seawater Sr/Ca (and Ba/Ca) ratios (e.g. Balter et al., 2011), as well as oxygen isotope composition and  $^{87}\text{Sr}/^{86}\text{Sr}$  ratios (e.g. Kocsis et al., 2009; Fischer et al., 2012). Shark teeth are an ideal geochemical archive because of their large temporal range (Devonian to present) and their resistance to diagenetic alteration (Reynard et al., 1999). Previous studies by Skulan and DePaolo (1999) and Martin et al. (2015) suggest that both seawater  $\delta^{44/40}\text{Ca}$  values and trophic level contribute to shark teeth enamel  $\delta^{44/40}\text{Ca}$  values, suggesting that variations in the  $\delta^{44/40}\text{Ca}_{\text{sw}}$  should be recorded in fossil shark teeth.

Here we present a large compilation of both modern ( $N = 100$ ) and fossil ( $N = 385$ ) shark teeth that have been analyzed for  $\delta^{44/40}\text{Ca}$ ,  $^{87}\text{Sr}/^{86}\text{Sr}$ , and Sr/Ca ratios to reconstruct these geochemical properties of seawater over the last 100 million years. Despite wide ranges at each time interval, our records indicate that the  $\delta^{44/40}\text{Ca}$  of seawater has increased since the Mesozoic and seawater Sr/Ca concentrations have declined by a factor of 1.5 to 2. We show that these changes can be explained by a reduction in the volume of diagenetically-altered shallow-water marine carbonates that is tied to the expansion of pelagic calcification in the mid-Mesozoic.

## 2. Materials and methods

### 2.1. Sample suite

Our sample suite consists of 100 modern teeth collected from specimens in the Atlantic, Pacific and Indian ocean basins (Fig. 1) representing 15 distinct genera (Fig. 2), including *Carcharhinus* ( $N = 27$ ), *Galeocerdo* ( $N = 15$ ), *Isurus* ( $N = 10$ ) and *Sphyrna* ( $N = 8$ ). These samples span a range of feeding ecologies, with trophic positions from 3.2 to 4.9 following FishBase classification (Froese and Pauly, 2019; Fig. 3). The sample suite also includes 6 specimens from bull sharks (*Carcharhinus leucas*), a species with the ability to migrate between freshwater and marine environments. A complete list of sample locations, genera and trophic level can be found in the supplemental file (Table S1).

Fossil teeth analyzed consist of 385 individual specimens from more than 30 different localities that span the Cretaceous to the Pleistocene. Samples were acquired from museum collections at the Smithsonian Institution National Museum of Natural History (Washington D.C, USA) and The Academy of Natural Sciences of Drexel University (Philadelphia, USA), and private collections from field sites in Morocco, Kazakhstan, California and South Carolina. Sample localities include the Lee Creek Mine (Miocene to Pliocene, North Carolina, USA), Calvert Cliff Formation (Miocene, Chesapeake Bay, Maryland, USA), the Phosphate Series of Morocco (late Cretaceous – early Eocene), the Austin Chalk Formation (Cretaceous, Texas, USA), Big Brook (Cretaceous, New Jersey, USA) and Cretaceous aged deposits in Mississippi (USA) amongst others (Fig. 1). The fossil sample suite spans 25 genera, including *Isurus* ( $N = 144$ ), *Scapanorhynchus* ( $N = 43$ ), *Odontaspis* ( $N = 42$ ), *Carcharodon* ( $N = 31$ ), and *Squalicorax* ( $N = 23$ ).

A complete summary of ages, genera, locations, loaning institutions and trophic classifications (where known) of fossil specimens is given in Table S2.

### 2.2. Sample preparation

At Princeton University, enameloid was isolated using a hand-held Dremel fit with a diamond wheel. Structurally, as fluorapatite, enameloid is understood to be more resistant to alteration than dentine due to a tighter crystal structure and is thus favorable for geochemical reconstructions (Reynard et al., 1999). A minimum of 1 mg of enameloid powder was dissolved in concentrated (16N) nitric acid. An aliquot of the dissolved sample was analyzed for major/minor/trace elements and the remainder dried down on a hotplate and dissolved in 0.2% nitric acid for column chromatography and isotopic analysis. Both Ca and Sr were purified for isotopic analysis using an automated ion chromatography system (Thermo Dionex IC-5000<sup>+</sup>) utilizing methanesulfonic acid as the eluent and a CS16 5 × 250 mm cation-exchange column (Blättler and Higgins, 2017; Higgins et al., 2018 and references therein).

At Rutgers University, sample powders were extracted from shark teeth using a dental drill and were cleaned for trace metal analysis following the protocol of (Boyle and Keigwin, 1985) without the reductive step. The cleaned powders were progressively reacted with trace metal grade 0.065N nitric acid until complete dissolution was achieved. After a 10 minute centrifugation, 100  $\mu\text{l}$  of the sample solution was further diluted with 300  $\mu\text{l}$  0.5N nitric acid to obtain a final Ca concentration of  $\sim 4\text{--}5$  mM to minimize matrix effects.

### 2.3. $\delta^{44/40}\text{Ca}$ analyses

Calcium isotopic analyses were carried out at Princeton University on a Thermo Scientific Neptune Plus multi-collector inductively coupled plasma mass spectrometer (MC-ICP-MS) using

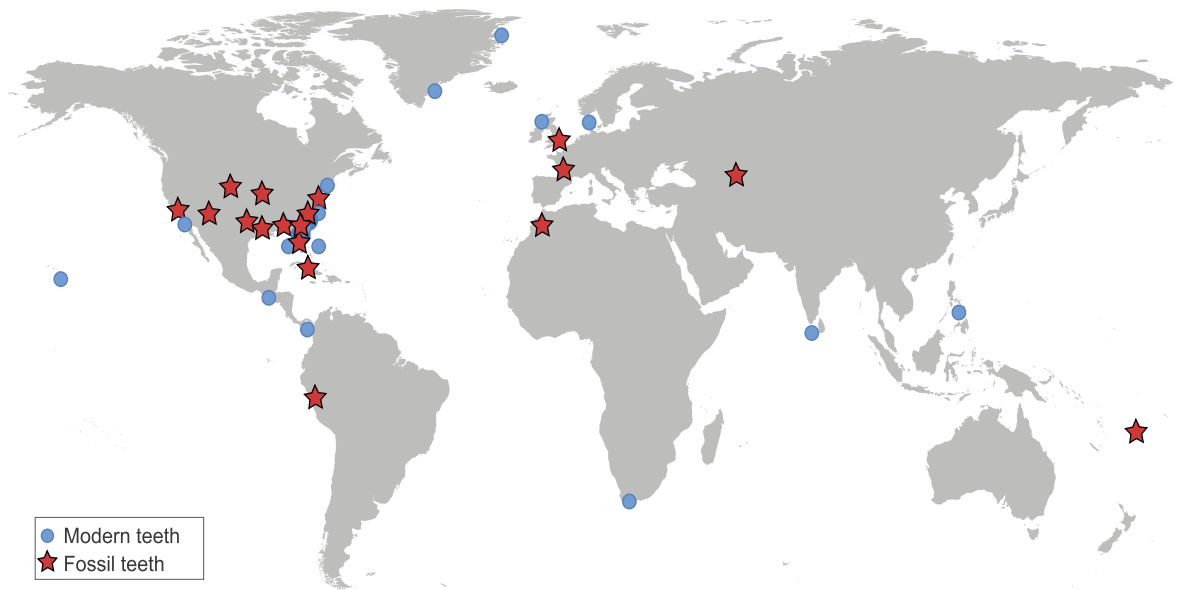


**Fig. 1.** World map showing distribution of locations from which samples were collected. Fossil specimen (Cretaceous to Pleistocene) locales are denoted by stars, while the circles correspond to modern sampling sites.

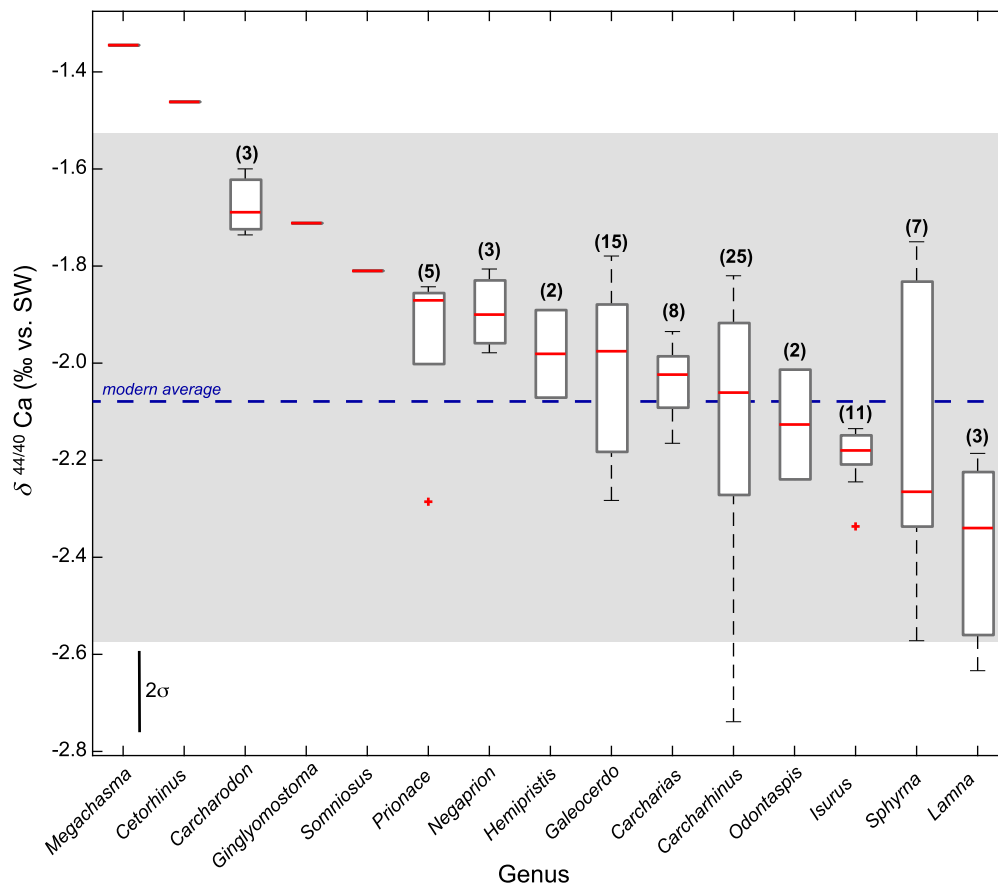


**Fig. 2.** Ca isotopic composition of modern shark teeth, arranged by genera. The full range of modern variability in  $\delta^{44/40}\text{Ca}$  is captured in several genera, most notably *Carcharhinus* and *Sphyrna*. Numbers in parenthesis represent individual specimens analyzed.

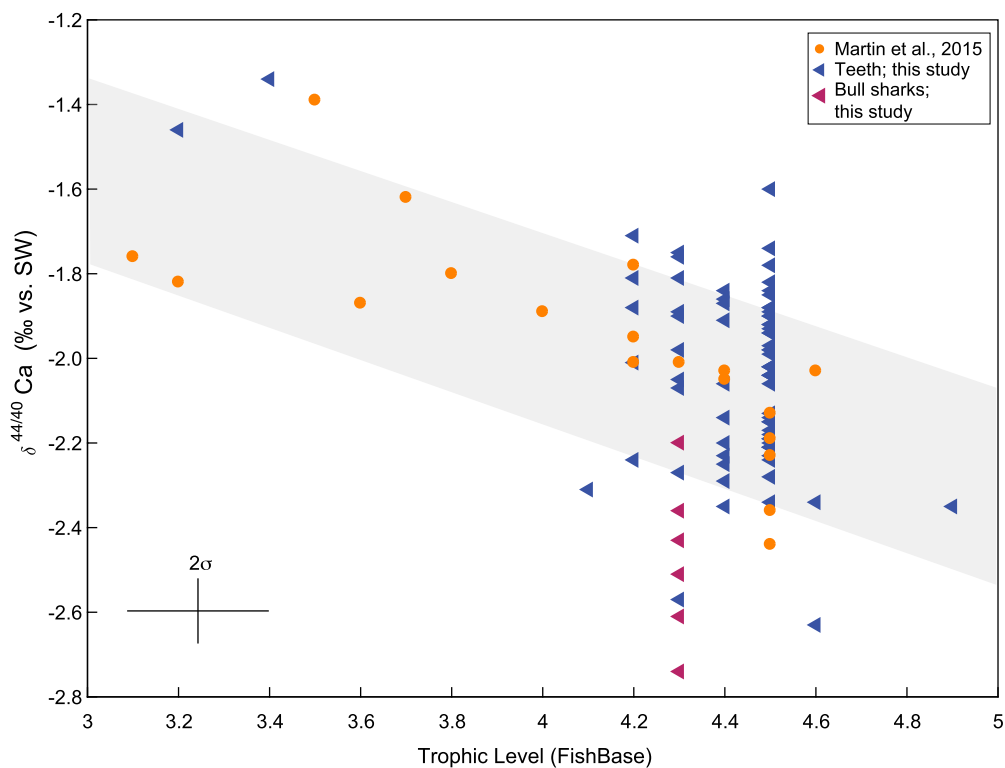


**Fig. 3.** Calcium isotopic composition of modern shark teeth arranged by trophic level from Fishbase (Froese and Pauly, 2019). Samples from this study are represented by triangles (including bull sharks - *Carcharhinus leucas* - in magenta) while orange circles represent data from Martin et al. (2015). An overall decrease in  $\delta^{44/40}\text{Ca}$  is observed with increasing trophic level. Average  $2\sigma$  of trophic levels is  $\pm 0.3$ . (For interpretation of the colors in the figure(s), the reader is referred to the web version of this article.)

an ESI Apex-IR inlet system following previously published protocols (Blättler and Higgins, 2017; Higgins et al., 2018 and references therein). Measurements were carried out at medium resolution to avoid ArHH<sup>+</sup> interferences on <sup>42</sup>Ca. Measured  $\delta^{44/42}\text{Ca}$  values were converted to  $\delta^{44/40}\text{Ca}$  assuming mass dependent fractionation and no excess radiogenic <sup>40</sup>Ca (Fantle and Tipper, 2014). Corrections are made for isobaric Sr<sup>2+</sup> interferences by using measurements at  $m/z = 43.5$ , representing doubly charged <sup>87</sup>Sr<sup>2+</sup>. Mass-dependence is verified using a three isotope plot ( $\delta^{44/42}\text{Ca}$  vs.  $\delta^{44/43}\text{Ca}$ ) and all measured data fall along a slope of 0.513, similar to the 0.507 slope predicted by the exponential mass-dependent fractionation law.

Ca isotope values are reported using delta notation relative to modern seawater ( $\delta^{44/40}\text{Ca}_{\text{seawater}} = 0\text{‰}$ ):

$$\delta^{44/40}\text{Ca}_{\text{seawater}} = \left( \frac{^{44}\text{Ca}/^{40}\text{Ca}_{\text{sample}}}{^{44}\text{Ca}/^{40}\text{Ca}_{\text{seawater}}} - 1 \right)$$

$\delta^{44/40}\text{Ca}_{\text{seawater}}$  is  $+1.92\text{‰}$  on the SRM 915a scale and  $+0.98\text{‰}$  on the bulk silicate earth (BSE) scale (Fantle and Tipper, 2014). The accuracy and precision of our method is estimated from replicate purification and isotopic analyses of SRM 915b and an in-house shark tooth standard (JAWS) with each set of samples. Measured  $\delta^{44/40}\text{Ca}$  values for SRM 915b are  $-1.18 \pm 0.16\text{‰}$  ( $2\sigma$ ;  $N = 70$ ), indistinguishable from reported values of  $-1.16 \pm 0.08\text{‰}$  (Heuser and Eisenhauer, 2008) and  $-1.13 \pm 0.04\text{‰}$  (Jacobson et al., 2015). Measured isotopic composition for JAWS is  $-1.92 \pm 0.20\text{‰}$  ( $2\sigma$ ;  $N = 36$ ).

#### 2.4. <sup>87</sup>Sr/<sup>86</sup>Sr analysis

Strontium isotope analyses of shark tooth enameloid were used to refine the chronology of our sample suite and as a test of diagenetic alteration. Measured <sup>87</sup>Sr/<sup>86</sup>Sr values were converted to sample ages using the LOWESS seawater curve (McArthur et al., 2001). In all but 15 of the samples analyzed, the <sup>87</sup>Sr/<sup>86</sup>Sr age of

the sample agreed with stratigraphic age estimates. Samples where <sup>87</sup>Sr/<sup>86</sup>Sr derived ages differed from stratigraphic age constraints were excluded from further consideration.

<sup>87</sup>Sr/<sup>86</sup>Sr analyses were carried out on a Thermo Scientific Neptune Plus MC-ICP-MS at Princeton University in low mass resolution using a cyclonic spray chamber. Each sample consists of  $\sim 400$  ng of Sr analyzed in two aliquots at a concentration of 150 ppb. The accuracy and precision of these analyses are estimated from repeat analyses of NIST 987 and modern seawater purified through column chromatography. Measured seawater <sup>87</sup>Sr/<sup>86</sup>Sr values, normalized to a NIST 987 value of 0.71025 (McArthur et al., 1994), are  $0.709177 \pm 0.000045$  ( $2\sigma$ ,  $N = 34$ ).

#### 2.5. Major/minor/trace element analyses

Concentration analyses of major/minor/trace elements (e.g. Mg/Ca, Sr/Ca, Na/Ca) were carried out on either a Thermo Finnigan Element-2 inductively coupled plasma mass spectrometer (ICP-MS) or an ICP-OES (iCap-Q, Thermo) at Princeton University ( $N = 244$ ) or via Element XR ICP-MS at Rutgers University ( $N = 48$ ). At Princeton, metal to Ca (Me/Ca) ratios of samples were determined using a set of matrix-matched in-house calibration standards. External reproducibility of these measurements is estimated at  $\sim 10\%$  ( $2\sigma$ ) based on replicate measurements of SRM88b (dolomitic limestone) and an in-house shark tooth standard (JAWS). Sr/Ca analyses at Rutgers University followed the method of Rosenthal et al. (1999). Typical precision for Sr/Ca measurements was  $< 1\%$ .

### 3. Results

#### 3.1. $\delta^{44/40}\text{Ca}$ values of modern shark teeth

A histogram of measured  $\delta^{44/40}\text{Ca}$  values in modern shark tooth enamel ( $N = 85$ ) is shown in Fig. 4B. The average  $\delta^{44/40}\text{Ca}$  value

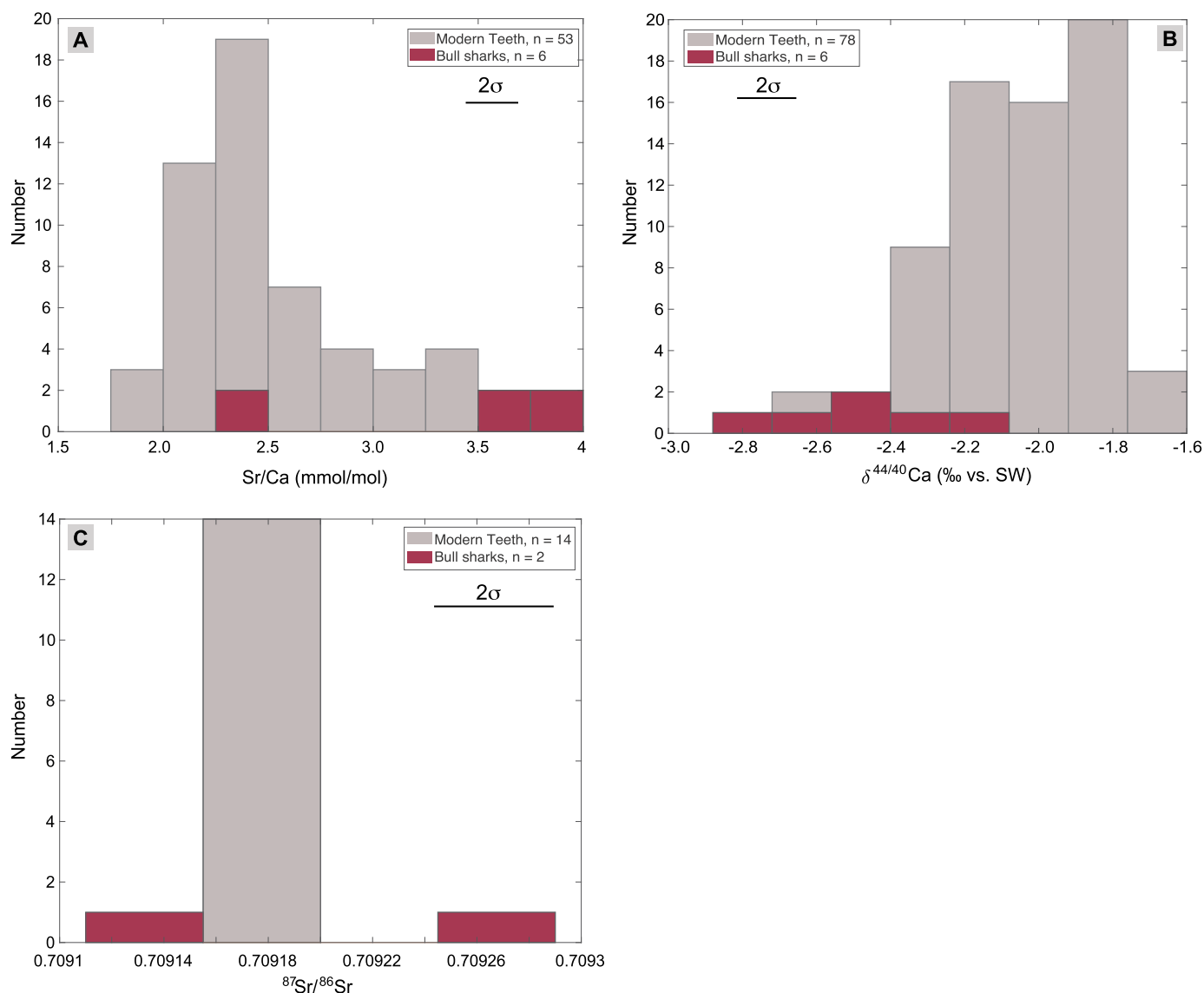


**Fig. 4.** (A) Histogram of  $\delta^{44/40}\text{Ca}$  for all modern shark teeth analyzed in this study. Specimens represent 15 genera, including *Carcharhinus leucas* (bull sharks). Excluding *C. leucas*, the average for modern teeth is  $-2.07\%$ . The large range observed (approaching  $1\%$ ) may be due to inter- and intra- genus variations. (B) Histogram of Sr/Ca (mmol/mol) for modern teeth. Bull sharks (*C. leucas*) are shown in magenta and represent some of the highest observed Sr concentrations. Excluding the bull shark data, across 9 measured genera, we observe an average Sr/Ca of  $2.45 \pm 0.79$  mmol/mol ( $2\sigma$ ,  $N = 46$ ). (C) Histogram of  $^{87}\text{Sr}/^{86}\text{Sr}$  for modern teeth. Bull sharks (*C. leucas*) are shown in magenta and represent the most enriched and depleted values respectively.  $^{87}\text{Sr}/^{86}\text{Sr}$  for modern seawater is 0.70918, indistinguishable from the modern tooth average.

of the full data set is  $-2.06 \pm 0.51\%$  ( $2\sigma$ ) compared to modern seawater and the range in values is  $>1\%$  ( $-1.34\%$  to  $-2.74\%$ ). Bull sharks (*Carcharhinus leucas*) are characterized by particularly low  $\delta^{44/40}\text{Ca}_{\text{tooth}}$  values (avg.  $\delta^{44/40}\text{Ca} = -2.47\%$ ;  $N = 6$ ) but otherwise there is broad overlap in  $\delta^{44/40}\text{Ca}$  values between the different shark species (Fig. 2). *Sphyrna* ( $N = 7$ ) and *Carcharhinus* ( $N = 25$ ) exhibit a large range in  $\delta^{44/40}\text{Ca}_{\text{tooth}}$  values, spanning the full range of variability observed in modern samples (from  $-1.75$  to  $-2.73\%$ ). *Isurus* ( $N = 11$ ) and *Carcharias* ( $N = 8$ ) exhibit narrower ranges, from  $-2.13$  to  $-2.33\%$  and  $-1.93$  to  $-2.17\%$  respectively. Measured  $\delta^{44/40}\text{Ca}$  values of six pairs of enamel and dentine indicate that  $\delta^{44/40}\text{Ca}$  values of dentine are elevated by an average of  $\sim 0.2\%$  compared to enamel (Table 1).

### 3.2. $\delta^{44/40}\text{Ca}$ values of fossil shark teeth

Measured  $\delta^{44/40}\text{Ca}_{\text{tooth}}$  values of fossil shark teeth ( $N = 247$ ) range from  $-1.48$  to  $-4.08\%$ . When plotted vs. sample age as determined by Sr isotopes and/or sequence stratigraphy,  $\delta^{44/40}\text{Ca}_{\text{tooth}}$

are lower in the Cretaceous and early Cenozoic and increase towards the present (Fig. 5A). Binning the data into 10 million-year intervals (red circles, Fig. 5A) reveals that  $\delta^{44/40}\text{Ca}_{\text{tooth}}$  values increase by  $\sim 0.5\%$ , with much of this increase occurring over the last  $\sim 50$  Ma. Each bin contains samples from between 3 and 10 different shark species and the variability in  $\delta^{44/40}\text{Ca}_{\text{tooth}}$  within each time bin ( $2\sigma$  between  $0.37\%$  and  $0.69\%$ ; represented by the vertical error bars in Fig. 5A) is similar to the modern ( $2\sigma = 0.51\%$  for entire data set or  $0.4\%$  excluding bull sharks). The use of 10 Ma bins allows for a time-averaged reconstruction of seawater properties. For example, comparison of the time bins 0-10 Ma and 60-70 Ma clearly indicates that while both bins exhibit variability that is comparable to that observed in the modern, the mean of the inferred seawater  $\delta^{44/40}\text{Ca}$  values for the 60-70 Ma bin is lower than the 0-10 Ma bin by  $0.33\%$  ( $-0.41\%$  versus  $-0.08\%$ ).

To evaluate the significance of the observed increase in tooth  $\delta^{44/40}\text{Ca}$  values, a randomized synthetic data series (10,000 simulations) of  $\delta^{44/40}\text{Ca}$  was generated using a mean of  $0\%$  and a  $2\sigma$  of

**Table 1**  
Results of Ca isotope analyses on enamel - dentine pairs from 7 modern individuals.

Genus	Location	$\delta^{44/40}\text{Ca}$ (‰ vs. SW) enamel	$\delta^{44/40}\text{Ca}$ (‰ vs. SW) dentine	$\Delta_{\text{enamel-dentine}}$
<i>Carcharhinus</i>	Florida	-2.51	-2.21	-0.30
<i>Carcharhinus</i>	Florida	-1.97	-1.81	-0.16
<i>Carcharhinus</i>	Panama	-1.88	-1.79	-0.09
<i>Sphyrna</i>	Florida	-1.76	-1.54	-0.21
<i>Carcharhinus</i>	Florida	-2.14	-1.78	-0.36
<i>Negaprion</i>	Florida	-1.81	-1.78	-0.03
<i>Galeocerdo</i>	Florida	-1.90	-1.71	-0.19

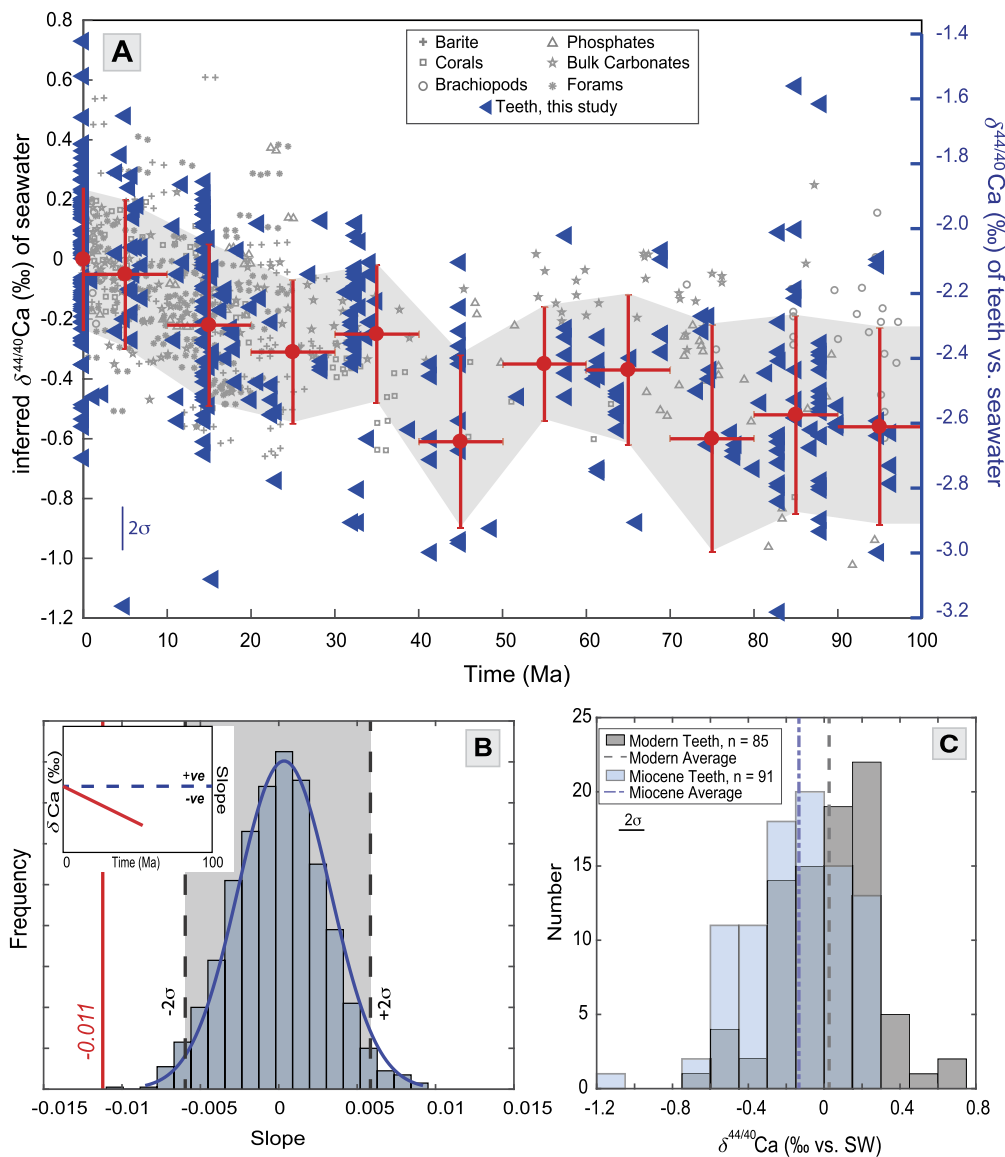


**Fig. 5.** (A) Late Mesozoic and Cenozoic record of seawater  $\delta^{44/40}\text{Ca}$  from shark teeth (blue triangles). Inferred seawater  $\delta^{44/40}\text{Ca}$  is calculated by adding the modern average ( $-2.06\text{‰}$ ) to the absolute measurements (shown on secondary y-axis). Moving mean with 10 million year bins is calculated for tooth data and shown in red circles, with vertical error bars representing  $2\sigma$  for each bin. Grey highlighted region represents possible inferred range of seawater  $\delta^{44/40}\text{Ca}$ . Reconstruction includes measurements of corals (Gothmann et al., 2016), brachiopods (Farkaš et al., 2007), phosphates (Soudry et al., 2006), deep-sea bulk carbonates (Fantle and DePaolo, 2005, 2007; Gothmann et al., 2016) and marine barite (Griffith et al., 2008). (B) Histogram of 10,000 iterations of calculated slope for randomly generated  $\delta^{44/40}\text{Ca}_{\text{sw}}$  change over the Cenozoic (Monte Carlo simulation). Dashed lines represent bounds of  $2\sigma$  uncertainty. The slope derived from shark tooth  $\delta^{44/40}\text{Ca}_{\text{sw}}$  reconstructions since 50 Ma in (A) falls outside the  $2\sigma$  range, indicating that the observed enrichment is not an artifact of randomness and/or noise. (inset) Schematic representation of calculation in (B). Null hypothesis, assuming no change in  $\delta^{44/40}\text{Ca}_{\text{sw}}$  since the Cretaceous, would result in a slope of 0 (blue dashed line). Isotopic enrichment since 50 Ma, as observed in (A), gives rise to the negative, non-zero slope as shown in (B). (C) Histogram comparing inferred  $\delta^{44/40}\text{Ca}_{\text{sw}}$  from modern and Miocene-aged shark teeth with averages of  $0.02\text{‰}$  and  $-0.15\text{‰}$ , respectively. Student's  $t$ -test suggests that the difference between these populations is statistically significant  $t(174) = 4.36$ ,  $p < 0.001$ . (For interpretation of the colors in the figure(s), the reader is referred to the web version of this article.)

0.4‰, after the modern tooth compilation excluding *C. leucas*. We assume that any trophic-level or intra-trophic level variability remains constant with time. Using averages of 10-million-year time bins of the randomized data, we calculate slopes for the change of seawater  $\delta^{44/40}\text{Ca}$  over the last ~65 Ma. As shown in Fig. 5B, these slopes all converge to 0, with a  $2\sigma$  of  $\pm 0.0058$  ‰/yr. The best-fit slope representing the rate of change in inferred  $\delta^{44/40}\text{Ca}$  of seawater over the last 65 Ma is  $-0.011$ ‰/Ma, indicating that the observed increase in  $\delta^{44/40}\text{Ca}_{\text{tooth}}$  values is statistically significant (Fig. 5B).

### 3.3. Sr/Ca ratios and $^{87}\text{Sr}/^{86}\text{Sr}$ of modern shark teeth

A histogram of measured Sr/Ca ratios in modern shark tooth enamel is shown in Fig. 4A. Across 10 measured genera, we observe an average Sr/Ca of  $2.54 \pm 0.99$  mmol/mol ( $2\sigma$ ,  $N = 59$ ). A subset of measured bull sharks (*C. leucas*) exhibit the highest Sr concentrations, on average  $3.31 \pm 1.43$  mmol/mol ( $2\sigma$ ;  $N = 6$ ), in agreement with previous studies on this species ( $3.31 \pm 0.52$  mmol/mol;  $2\sigma$ ;  $N = 49$ ) (Kocsis et al., 2015). For genera with  $\geq 5$  measured specimens (i.e. *Carcharhinus*, *Carcharias*, *Galeocerdo*, and *Isurus*), the average is  $2.60 \pm 0.36$  mmol/mol ( $2\sigma$ ,  $N = 41$ ), with *Carcharias* exhibiting the lowest Sr concentrations ( $2.34 \pm 0.19$  mmol/mol;  $2\sigma$ ,  $N = 7$ ).

A histogram of measured  $^{87}\text{Sr}/^{86}\text{Sr}$  in modern shark tooth enamel ( $N = 16$ ) is shown in Fig. 4C. Across 8 measured genera, we observe an average  $^{87}\text{Sr}/^{86}\text{Sr}$  of  $0.709180 \pm 0.000042$  ( $2\sigma$ ), indistinguishable from modern seawater (0.709177; McArthur et al., 2001). Two measured bull sharks (*C. leucas*) exhibit the highest and lowest observed values, 0.709251 and 0.709152 respectively.

### 3.4. Sr/Ca ratios of fossil shark teeth

Measured Sr/Ca ratios of our suite of fossil shark teeth ( $N = 232$ ) range from 1.00 to 5.75 mmol/mol. When plotted vs. sample age as determined by Sr isotopes and/or sequence stratigraphy there is an observed two-fold decrease in the Sr/Ca of teeth since the late Cretaceous, from ~5 mmol/mol to the modern value of 2.5 mmol/mol (Fig. 6A).

We reconstruct seawater Sr/Ca concentrations from measured Sr/Ca ratios in fossil shark teeth using a partition coefficient ( $K_D = (\text{Sr}/\text{Ca})_{\text{tooth}}/(\text{Sr}/\text{Ca})_{\text{seawater}}$ ) calculated from modern elasmobranch enameloid (2.55 mmol/mol,  $N = 59$ ) and seawater (8.6 mmol/mol; Tripathi et al., 2009) and ignoring the impact of temperature. The resulting  $K_D$  of ~0.3 is similar to that determined for abiotic apatite at 25°C (Balter and Lécuyer, 2004). We justify ignoring the influence of temperature based on the results shown in Fig. 7 where enameloid Sr/Ca shows no relationship with latitude, used here as a proxy for water temperature. Our fossil tooth record for seawater Sr/Ca ratios is in general agreement with other biogenic carbonate-based records of seawater Sr/Ca e.g. corals (Ivany et al., 2004; Griffiths et al., 2013; Gothmann et al., 2015); benthic forams (Lear et al., 2003); gastropods (Tripathi et al., 2009; Sosdian et al., 2012); elasmobranch teeth (Balter et al., 2011), and suggests a  $2\times$  higher concentration of marine Sr/Ca in the Cretaceous (~15 mmol/mol) compared to present day (8.6 mmol/mol).

Reconstructions of the  $[\text{Sr}]_{\text{sw}}$  using the Sr/Ca record and a linear regression of  $[\text{Ca}]_{\text{sw}}$  reconstructions from fluid inclusions in marine evaporite minerals (Horita et al., 2002; Lowenstein et al., 2003) (Fig. 6 B and C) indicates a four-fold decrease in  $[\text{Sr}]_{\text{sw}}$  over the last 100 Ma (Fig. 6C).

## 4. Discussion

Measured  $\delta^{44/40}\text{Ca}$  values and Sr/Ca ratios in both modern and ancient elasmobranch tooth enamel may contain information on

elasmobranch diet, physiology, or temperature, which may complicate and/or obscure inferences of secular variability in the  $\delta^{44/40}\text{Ca}$  or Sr/Ca of seawater on geologic timescales. Indeed, the large (~1‰) variability in  $\delta^{44/40}\text{Ca}$  values in modern elasmobranch tooth enamel indicates that the isotopic effects of diet and physiology are as large as putative changes in the  $\delta^{44/40}\text{Ca}$  of seawater. In the following sections we discuss the source of this variability and how it affects interpretations of secular change in the  $\delta^{44/40}\text{Ca}$  and Sr/Ca of seawater from measurements in fossil elasmobranch tooth enamel. In spite of these uncertainties, we conclude that first-order changes in the average  $\delta^{44/40}\text{Ca}_{\text{tooth}}$  and Sr/Ca<sub>tooth</sub> in our dataset reflect changes in the  $\delta^{44/40}\text{Ca}$  and Sr/Ca of seawater. Finally, we quantitatively link the reconstructed changes in seawater  $\delta^{44/40}\text{Ca}$  and Sr/Ca to a decline in the deposition and early diagenetic alteration of shallow-water carbonate sediments associated with the expansion of the pelagic carbonate sink since the mid-Mesozoic.

### 4.1. Dietary and physiological controls on the $\delta^{44/40}\text{Ca}_{\text{tooth}}$ and the Sr/Ca<sub>tooth</sub> in elasmobranchs

Previous work on modern marine organisms has shown that the  $\delta^{44/40}\text{Ca}$  of biomineralized tissues (i.e. bones and enamel) declines with increasing trophic level (Skulan and DePaolo, 1999; Clementz et al., 2003; Martin et al., 2015). The trophic-level dependence results from fractionation of Ca isotopes during the formation of bone or cartilage, which preferentially incorporate  $^{40}\text{Ca}$ , leading to low  $^{44}\text{Ca}/^{40}\text{Ca}$  ratios in these tissues. As these tissues constitute the principle Ca reservoir in vertebrates and represent a major source of dietary Ca, the consumption and formation of bone and cartilage drives  $\delta^{44/40}\text{Ca}$  values lower with increasing trophic level. The magnitude of the effect, based on a single study of zooplanktivores to tertiary consumers ( $N = 18$ ), is ~0.3‰ per nominal trophic level (Martin et al., 2015).

Although the majority of our modern sample suite spans a narrow range of trophic levels (4.2 to 4.5 from Fishbase; Froese and Pauly, 2019), a small number of samples at both lower (3.1 and 3.2) and higher (4.6 and 4.9) levels indicates that the effect observed by Martin et al. (2015) persists in a much larger data set of elasmobranch teeth ( $N = 85$ , Fig. 3). Furthermore, assuming the offset between trophic levels remains constant through time (i.e. an expected 0.3‰ depletion per nominal trophic level), a change in the  $\delta^{44/40}\text{Ca}$  of seawater would translate across the entire trophic chain. Barring any large shifts in elasmobranch feeding ecologies since the Cenozoic, e.g. all tertiary consumers shifting to feeding at a lower level, the observed enrichment in the  $\delta^{44/40}\text{Ca}$  can only be reflective of changes in the composition of seawater. However, we also observe significant Ca isotopic variability within trophic levels. For example, trophic status for *Carcharhinus* ( $N = 25$ ) and *Galeocerdo* ( $N = 14$ ) span a narrow range (4.2 to 4.5) whereas  $\delta^{44/40}\text{Ca}_{\text{tooth}}$  values vary between individuals by as much as ~1‰ and ~0.5‰, respectively. This variability is not necessarily true of all genera, as teeth from *Isurus* ( $N = 11$ ) are indistinguishable in their Ca isotopic composition (with an observed spread within the long-term external reproducibility of the measurement) (Fig. 2).

Variability in modern  $\delta^{44/40}\text{Ca}_{\text{tooth}}$  values at the genus level may result from either seasonality of dietary composition, physiology, or, in the case of bull sharks (*C. leucas*), differences in the  $\delta^{44/40}\text{Ca}$  value of seawater and freshwater habitats. With regards to diet, given the relatively short period of time (~weeks to months, depending on species) sampled by an individual tooth (Zeichner et al., 2017), the variability may reflect differences in both the isotopic composition and abundance of Ca in different sources (e.g. marine mammals vs. cartilaginous teleosts). Transport of Ca from seawater across the gills constitutes an important but poorly constrained additional source of Ca. Estimates of the magnitude of this source in teleosts indicate that it may constitute up to ~70% of to-

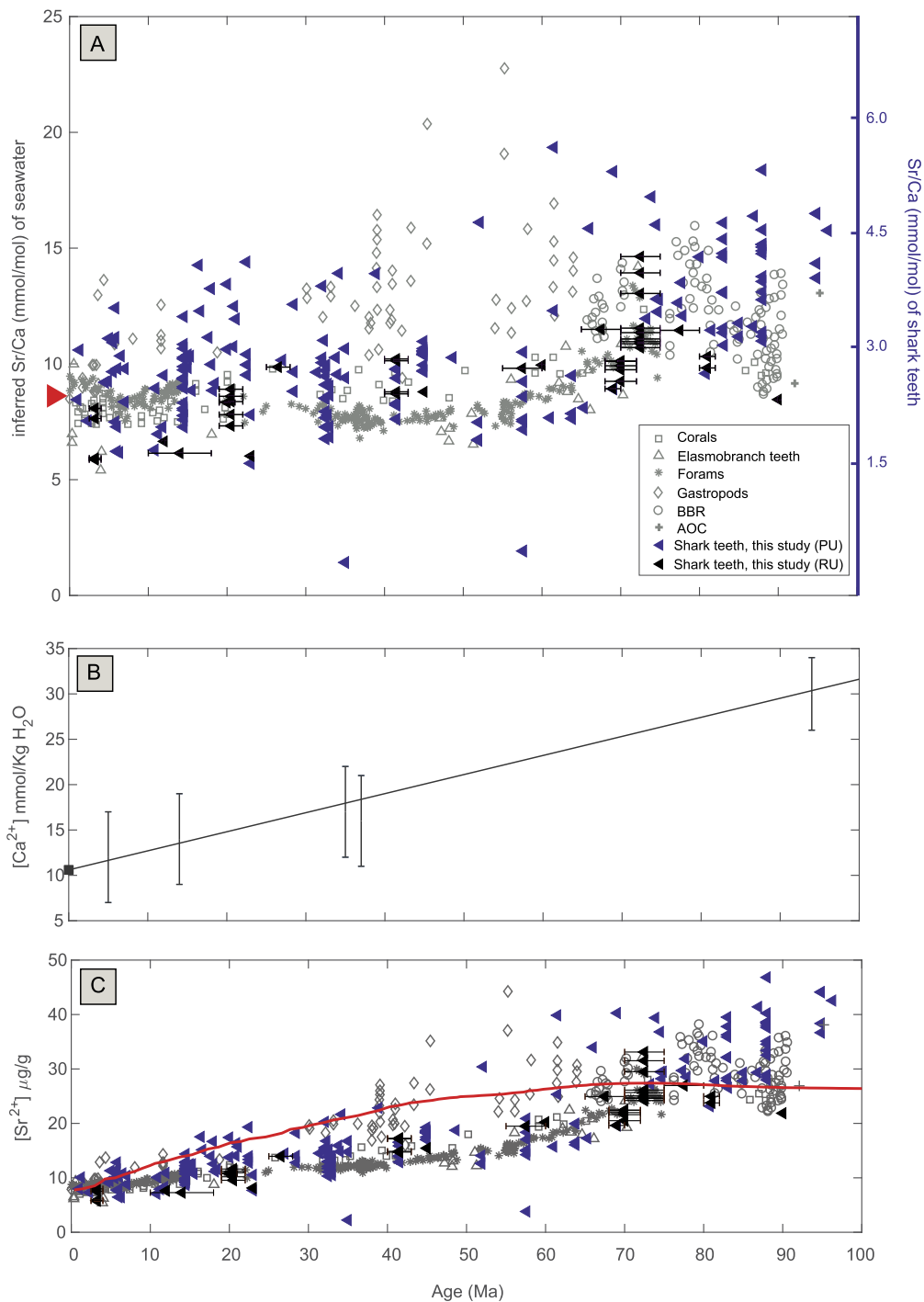


**Fig. 6.** (A) Reconstruction of paleoseawater Sr/Ca (mmol/mol) from shark teeth (triangles, this study), and elasmobranch teeth (Balter et al., 2011), corals (Ivany et al., 2004; Griffiths et al., 2013; Gothmann et al., 2015), benthic forams (Lear et al., 2003), gastropods (Tripathi et al., 2009; Sosdian et al., 2012), BBR (brachiopods, belemnites and rudists; Steuber and Veizer, 2002) and altered oceanic crust (Coogan, 2009). In agreement with other records, shark teeth suggest an elevated seawater Sr/Ca in the late Cretaceous (~15 mmol/mol) compared to present day. Modern seawater (8.6 mmol/mol, Tripathi et al., 2009) is indicated by the red arrow. (B) Estimation of seawater Ca concentration based on fluid inclusions in evaporites (Horita et al., 2002; Lowenstein et al., 2003) and a linear regression forced through the modern seawater Ca concentration. (C) Paleoseawater Sr concentrations calculated from combining Sr/Ca data from (A) with seawater Ca estimate in (B) suggests a four-fold decrease in [Sr]<sub>sw</sub> since the late Cretaceous. Preferred-fit model output for reconstructions of [Sr]<sub>sw</sub> is represented by the red line (Section 4.4.2) and calculated using variables listed in Table 2.

tal Ca (Sundell and Björnsson, 1988). Fractionation of Ca isotopes during transport across the gills is currently unknown. However, recent studies on terrestrial mammals have shown that biological processing of Ca is associated with isotopic fractionation (e.g. re-absorption in the kidneys) leading to an elevated  $\delta^{44/40}\text{Ca}$  value in urine compared to diet (Heuser and Eisenhauer, 2010; Morgan et al., 2012; Tacail et al., 2014). Finally, as migratory elasmobranchs

with the ability to adapt to freshwater and marine environments, variability in the  $\delta^{44/40}\text{Ca}$  of bull sharks (*C. leucas*) may also reflect the large difference in  $\delta^{44/40}\text{Ca}$  values between seawater (0‰) and continental rivers (~-1‰). Accordingly, measured  $\delta^{44/40}\text{Ca}$  values of *C. leucas* teeth are systematically lighter than other modern teeth (average =  $-2.47 \pm 0.2\%$ ,  $2\sigma$ ; N = 6, Fig. 2A). With one exception, measured  $^{87}\text{Sr}/^{86}\text{Sr}$  ratios in a subset of these samples did not dif-

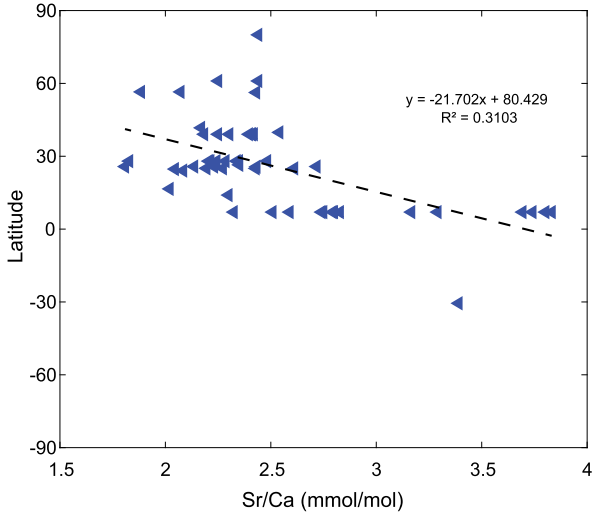


**Fig. 7.** Measured Sr/Ca for modern shark teeth plotted against latitude, used here as a proxy of water temperature, of sampling location (where known). Dashed red line represents best-fit linear regression with  $R^2 = 0.31$ .

fer significantly from modern seawater (Fig. 4C), an observation which may indicate that river had  $^{87}\text{Sr}/^{86}\text{Sr}$  ratios dominated by the weathering of recent carbonates (e.g. Florida Bay) or that other factors (e.g. trophic level) are required to explain the low  $\delta^{44/40}\text{Ca}$  values of bull sharks.

The partition coefficient ( $K_D$ ) determined for modern elasmobranch teeth in this study ( $\sim 0.3$ ) is similar to that determined experimentally for inorganic apatite (0.33; Balter and Lécuyer, 2004), suggesting the effects of physiology are small. The importance of diet, however, is poorly constrained. Based on studies of terrestrial mammals, environmental variability of Sr/Ca signals may be obscured by trophic level effects (Balter et al., 2011). The influence of temperature on  $K_D$  has been demonstrated experimentally. A range in  $K_D$  from 0.6 at  $5^\circ\text{C}$  to 0.237 at  $60^\circ\text{C}$  (Balter and Lécuyer, 2004) is observed, which translates to a Sr/Ca<sub>tooth</sub> range between 5.16 mmol/mol and 2.04 mmol/mol for modern seawater and could explain the range seen for modern teeth (Fig. 4A). However, for modern samples we observe variable and overlapping Sr/Ca<sub>tooth</sub> ratios for a range of water temperatures (as approximated by latitude) (Fig. 7). Indeed, cold-water *Somniosus microcephalus* from Greenland ( $\sim 3\text{--}6^\circ\text{C}$ ), and a sleeper shark (*Somniosidae sp.*) caught off the shores of Denmark, are associated with Sr/Ca ratios that are indistinguishable from warmer water species, including mako sharks (*Isurus sp.*) caught off the New Jersey coast ( $\sim 16\text{--}20^\circ\text{C}$ ) and other shark species caught along the Gulf Coast of Florida ( $\sim 30^\circ\text{C}$ ).

#### 4.2. The $\delta^{44/40}\text{Ca}_{\text{sw}}$ since 100 Ma

In spite of the uncertainties associated with elasmobranch diet and physiology, we interpret changes in the binned averages of our fossil  $\delta^{44/40}\text{Ca}_{\text{tooth}}$  values as recording a  $\sim 0.5\text{‰}$  increase in the  $\delta^{44/40}\text{Ca}_{\text{sw}}$  since 100 Ma (Fig. 5A) for three reasons.

First, as seawater Ca is the ultimate source of all of the Ca in the food chain, changes in the  $\delta^{44/40}\text{Ca}_{\text{sw}}$  should lead to similar changes in the  $\delta^{44/40}\text{Ca}$  of each trophic level. This will also be true of the  $\delta^{44/40}\text{Ca}$  of Ca sources associated with transport across the gills. Thus, as long as our dataset reflects a similar composition of trophic levels through time and accurately samples the natural variability in a given time interval, changes in the binned averages of our fossil  $\delta^{44/40}\text{Ca}_{\text{tooth}}$  values will reflect changes in  $\delta^{44/40}\text{Ca}_{\text{sw}}$ . The observation that variability in fossil  $\delta^{44/40}\text{Ca}_{\text{tooth}}$  values within each time bin ( $2\sigma$  between  $0.37\text{‰}$  and  $0.69\text{‰}$ ) is similar to the variability observed in modern teeth ( $2\sigma = 0.51\text{‰}$ ;  $0.4\text{‰}$  exclud-

ing *C. leucas*) suggests that the number of fossil samples analyzed in each time bin is sufficient to capture the natural variability in  $\delta^{44/40}\text{Ca}_{\text{tooth}}$  values for a given  $\delta^{44/40}\text{Ca}_{\text{sw}}$ .

Second, when we apply a genus-specific correction for  $\delta^{44/40}\text{Ca}_{\text{sw}}$  using *Isurus*  $\delta^{44/40}\text{Ca}_{\text{tooth}}$  values (modern average  $-2.19\text{‰}$ ,  $2\sigma = 0.12$ ,  $N = 11$ ) we find a similar  $\sim 0.5\text{‰}$  increase in the  $\delta^{44/40}\text{Ca}_{\text{sw}}$  since the late Mesozoic.

Third, alternative explanations for the  $\sim 0.5\text{‰}$  increase, for example a decline of two trophic levels in tertiary consumers, are inconsistent with independent observations of tooth morphology, suggesting that elasmobranch dietary habits have remained relatively static (Wilga et al., 2007).

Our record of an increase in  $\delta^{44/40}\text{Ca}_{\text{sw}}$  over the Cenozoic from fossil elasmobranch tooth enamel compares favorably with previous studies using barite (Griffith et al., 2008), brachiopods (Farkaš et al., 2007) and corals (Gothmann et al., 2016), though only the coral record of Gothmann et al. (2016) covers a similar time period (Fig. 5A). Gothmann et al. (2016) observed a  $\sim 1\text{‰}$  increase in the  $\delta^{44/40}\text{Ca}$  of fossil corals extending back to 160 Ma, with  $\sim 50\%$  of this increase occurring over the last  $\sim 60$  Ma. Although Gothmann et al. (2016) conclude that much of the increase in the  $\delta^{44/40}\text{Ca}$  of fossil corals since the Mesozoic could be attributed to coral vital effects, the strong agreement between both records suggests that an increase in the  $\delta^{44/40}\text{Ca}_{\text{sw}}$  can explain much (though likely still not all; see Gothmann et al., 2016) of the increase in the  $\delta^{44/40}\text{Ca}$  of fossil corals since the Triassic.

#### 4.3. The $[\text{Sr}]_{\text{sw}}$ since 100 Ma

We reconstruct  $[\text{Sr}]_{\text{sw}}$  from measured Sr/Ca ratios in fossil elasmobranch tooth enamel, appropriate partition coefficients (Section 3.4), and reconstructions of  $[\text{Ca}]_{\text{seawater}}$  from fluid inclusions in sedimentary evaporites (Horita et al., 2002; Lowenstein et al., 2003). Our record indicates that  $[\text{Sr}]_{\text{sw}}$  has declined by a factor of 4 since 100 Ma ( $\sim 36 \mu\text{g/g}$  to  $8.6 \mu\text{g/g}$ ; Fig. 6C), in agreement with other biogenic carbonate-based records including corals (Ivany et al., 2004; Griffiths et al., 2013; Gothmann et al., 2015), benthic forams (Lear et al., 2003), gastropods (Tripathi et al., 2009; Sossian et al., 2012), elasmobranch teeth (Balter et al., 2011) and estimates from hydrothermally altered oceanic crust from the Troodos ophiolite at  $\sim 90$  Ma (Coogan, 2009).

#### 4.4. What controls the $\delta^{44/40}\text{Ca}_{\text{sw}}$ and $[\text{Sr}]_{\text{sw}}$ on geologic timescales?

The global geochemical cycles of Ca and Sr in seawater reflect the balance between sources from the chemical weathering of silicate and carbonate rocks on the continents and in the oceanic crust and sinks in marine carbonate minerals (Stoll and Schrag, 1998; Zhu and Douglas Macdougall, 1998; Fantle and Tipper, 2014):

$$d\text{Ca}/dt = F_{\text{swx}} + F_{\text{cw}} + F_{\text{hyd}} - F_{\text{CB}} \quad (1a)$$

$$d\text{Sr}/dt = F_{\text{swx}} + F_{\text{cw}} + F_{\text{hyd}} - K_{\text{Sr/Ca}} \times [\text{Sr}]/[\text{Ca}]_{\text{sw}} \times F_{\text{CB}} \quad (1b)$$

where  $F_{\text{swx}}$ ,  $F_{\text{cw}}$ ,  $F_{\text{hyd}}$  and  $F_{\text{CB}}$  refer to fluxes of Ca and Sr from silicate weathering, carbonate weathering, hydrothermal alteration and carbonate burial respectively. The input flux terms (i.e., silicate weathering, carbonate weathering and hydrothermal alteration) may be combined into a single 'SOURCE' term that we assume remains constant. Our conclusions are not sensitive to this assumption because the isotopic composition of these sources is indistinguishable from bulk silicate Earth (Fantle and Tipper, 2014), and the flux from hydrothermal alteration is small relative to  $F_{\text{swx}}$  and  $F_{\text{cw}}$  (Elderfield and Schultz, 1996). The global Sr sink in carbonate sediments depends on  $[\text{Sr}]_{\text{sw}}$  and the average partition coefficient

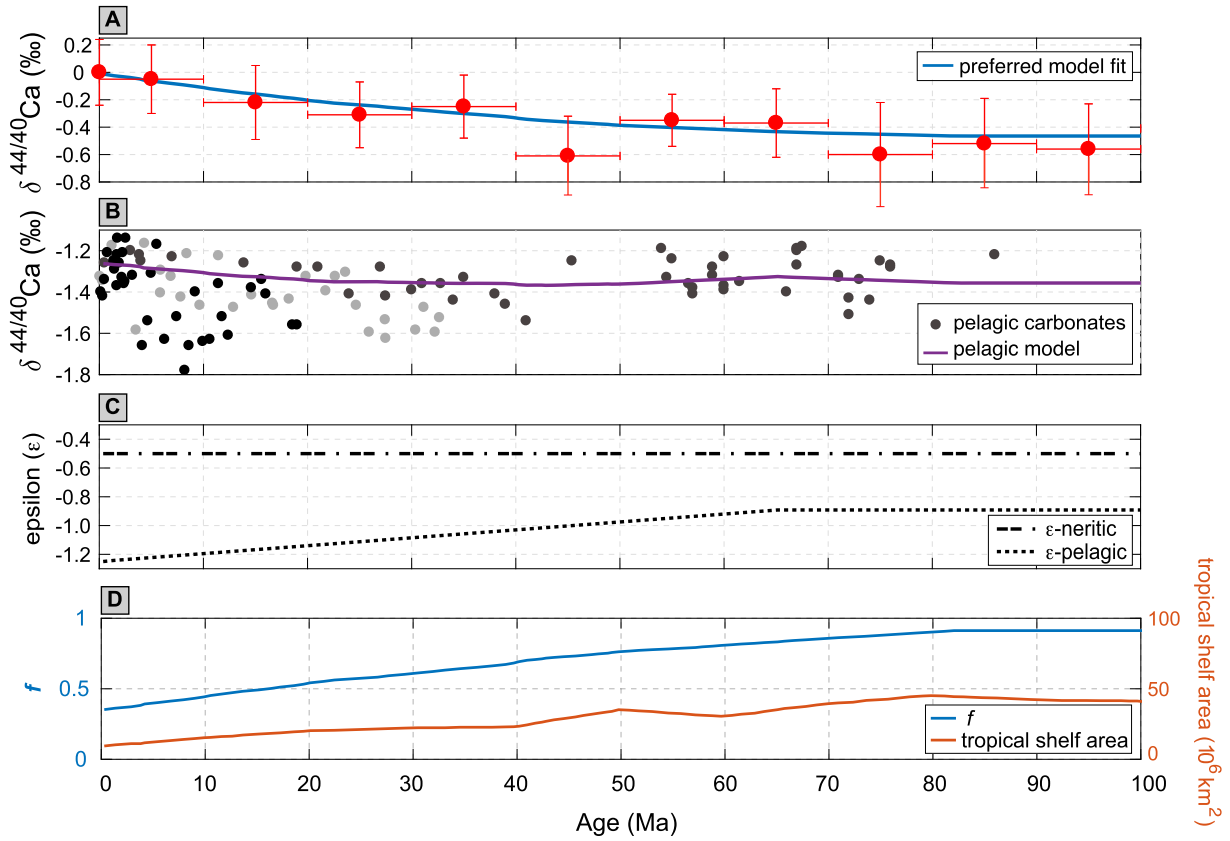


**Fig. 8.** (A) Preferred model fit prediction for seawater  $\delta^{44/40}\text{Ca}$  from Equation (3b) with values listed in Table 2. Moving mean with 10 Ma bins is calculated for tooth data and shown in red circles, with error bars representing  $2\sigma$  for each bin (as in Fig. 5A). (B) Measured  $\delta^{44/40}\text{Ca}$  of bulk pelagic carbonates (Fantle and DePaolo, 2005, 2007; Gothmann et al., 2016) that are used to estimate the  $\varepsilon_{\text{pelagic}}^{\text{Ca}}$  shown in (C). Note that the  $\delta^{44/40}\text{Ca}$  composition of pelagic sediments has remained constant over the Cenozoic. The pelagic model curve is calculated using the preferred model output for seawater  $\delta^{44/40}\text{Ca}$  shown in (A) and  $\varepsilon_{\text{pelagic}}^{\text{Ca}}$ . The reported  $2\sigma$  is between 0.05 and 0.3‰. (C) Estimates of  $\varepsilon_{\text{neritic}}^{\text{Ca}}$  and  $\varepsilon_{\text{pelagic}}^{\text{Ca}}$  used to calculate the preferred model fit for the  $\delta^{44/40}\text{Ca}$  of seawater shown in (A). The value for  $\varepsilon_{\text{pelagic}}^{\text{Ca}}$  is determined from the difference between the  $\delta^{44/40}\text{Ca}_{\text{seawater}}$  and  $\delta^{44/40}\text{Ca}_{\text{pelagic}}$ , where the former is taken from our fossil elasmobranch record and the latter from measurements of bulk pelagic carbonate over the Cenozoic (Fantle and DePaolo, 2005, 2007; Gothmann et al., 2016). Using this approach, we calculate an increase in  $\varepsilon_{\text{pelagic}}^{\text{Ca}}$  from 0.8‰ in the late Mesozoic to approximately 1.2‰ today. (D) Estimates of carbonate accumulation on platforms from Opdyke and Wilkinson (1988) are used to determine an approximate flux ( $f$ ) of carbonate sedimentation in platform (neritic) environments (blue line). This flux estimation is used to estimate the  $\delta^{44/40}\text{Ca}$  of seawater shown in (A). (For interpretation of the colors in the figure(s), the reader is referred to the web version of this article.)

( $K_{\text{Sr/Ca}}$ ) between seawater and carbonate sediments. Equation (1a) can be amended to reflect Ca isotope mass balance in seawater by including the isotopic composition of various Ca sources and average fractionation factors ( $\varepsilon \sim \delta^{44/40}\text{Ca}_{\text{sw}} - \text{avg. } \delta^{44/40}\text{Ca}_{\text{carb}}$ ) associated with global carbonate sink:

$$d\delta^{44/40}\text{Ca}/dt = F_{\text{swx}} + F_{\text{cw}} + F_{\text{hyd}} - (\delta^{44/40}\text{Ca}_{\text{sw}} - \varepsilon) \times F_{\text{CB}} \quad (1c)$$

where fluxes are the same as above, and  $\varepsilon$  represents the offset of  $\delta^{44/40}\text{Ca}$  of buried carbonates from  $\delta^{44/40}\text{Ca}_{\text{sw}}$ . When solved at steady-state (e.g.  $d\text{Sr}/dt = 0$ ), a reasonable assumption for both Sr and Ca for timescales longer than  $\sim 5$  million years, equations (1b) and (1c) reduce to:

$$[\text{Sr}]_{\text{sw}} = [\text{Ca}]_{\text{sw}} \times \text{SOURCE} / (D_{\text{Sr}} \times F_{\text{CB}}) \quad (2a)$$

$$\delta^{44/40}\text{Ca}_{\text{sw}} = \delta^{44/40}\text{Ca}_{\text{input}} + \varepsilon \quad (2b)$$

Equations (2a) and (2b) can be further modified to reflect the fact that the global carbonate sink is not uniform. Although there are many different ways to partition the global carbonate sink, a particularly useful paradigm for the last 100 million years is the partitioning of carbonate sinks between neritic and pelagic environments (Ridgwell, 2005):

$$[\text{Sr}]_{\text{sw}} = \text{SOURCE} - (D_{\text{neritic}}^{\text{Sr/Ca}} \times \text{Flux}_{\text{neritic}} + D_{\text{pelagic}}^{\text{Sr/Ca}} \times \text{Flux}_{\text{pelagic}}) \quad (3a)$$

$$\delta^{44/40}\text{Ca}_{\text{sw}} = \delta^{44/40}\text{Ca}_{\text{input}} - (f \times \varepsilon_{\text{neritic}}^{\text{Ca}} + (1 - f) \times \varepsilon_{\text{pelagic}}^{\text{Ca}}) \quad (3b)$$

where  $D_{\text{neritic}}^{\text{Sr/Ca}}$  and  $D_{\text{pelagic}}^{\text{Sr/Ca}}$  represent the single component distribution coefficient for neritic and pelagic carbonates and may be defined as the product of  $K^{\text{Sr/Ca}}$  and  $\text{Sr}/\text{Ca}_{\text{sw}}$ . The flux of Sr in neritic and pelagic carbonates is given in  $\text{Tmol/yr}$ . Calcium isotope fractionation factors for neritic and pelagic carbonates are given by  $\varepsilon_{\text{neritic}}^{\text{Ca}}$  and  $\varepsilon_{\text{pelagic}}^{\text{Ca}}$  respectively (Fig. 8C). The fractional flux ( $f$ ) of carbonate sedimentation in neritic environments is derived from estimates of carbonate accumulation on platforms and shown in Fig. 8D. The partitioning of the carbonate sink into neritic and pelagic components is done for three reasons. First, neritic and pelagic carbonate sediments have different sources – the former include metastable carbonate minerals such as aragonite and high-Mg calcite from a wide range of biogenic (e.g. corals), biologically mediated (e.g. stromatolites), and biologically ambiguous (e.g. micrite) sources whereas the latter are entirely biogenic in origin and composed primarily of low-Mg calcite in the form of coccoliths and foraminiferal tests. Second, there are systematic differences in the style and extent of diagenetic alteration in neritic and pelagic environments. Neritic environments

are often associated with fluid-buffered or open-system alteration that results in pervasive cementation, the formation of secondary dolomite (Ca,Mg)CO<sub>3</sub>, and wholesale re-setting of the chemistry of carbonate sediments (Swart and Melim, 2000; Melim et al., 2002; Swart and Eberli, 2005; Higgins et al., 2018). In contrast, carbonate diagenesis in pelagic environments occurs almost exclusively in sediment-buffered or closed-system conditions, where the potential to change the chemical composition of the sediment is limited (Richter and DePaolo, 1987; Fantle and DePaolo, 2006). Third, reconstructions of neritic shelf area indicate there have been changes in the partitioning of the global carbonate sink between neritic and pelagic environments over the last 100 Ma (Opdyke and Wilkinson, 1988; Walker et al., 2002; Ridgwell, 2005; van der Ploeg et al., 2019). In particular, tropical shelf area has declined four-fold since the Cretaceous, from  $40 \times 10^6$  km<sup>2</sup> to  $10 \times 10^6$  km<sup>2</sup>. At the same time, the radiation of planktonic calcifiers has shifted the mode of carbonate deposition to the deep ocean. Together, these effects have led to a six-fold decrease in neritic carbonate accumulation since the mid-Mesozoic (from  $0.6 \times 10^6$  km<sup>3</sup>/Ma to  $0.1 \times 10^6$  km<sup>3</sup>/Ma) (Opdyke and Wilkinson, 1988; Ridgwell, 2005).

#### 4.4.1. Mineralogy vs. diagenesis and the chemical composition of the neritic carbonate sink

Previous reconstructions of  $\delta^{44/40}\text{Ca}_{\text{sw}}$  over the Phanerozoic have attributed changes in composition to changes in the mineralogy of the neritic carbonate sink (e.g. aragonite vs. calcite; Farkaš et al., 2007). The reasons for this are twofold. First, Ca isotope fractionation in carbonate minerals has been shown to depend on mineralogy, with aragonite being preferentially enriched in <sup>40</sup>Ca compared to calcite (Gussone et al., 2005). Second, petrographic and geochemical reconstructions of carbonate mineralogy over the Phanerozoic have revealed systematic changes in the mineralogy of both inorganic and biogenic carbonate producers in neritic environments - the aragonite and calcite seas of Sandberg (1983) and Hardie (1996) - suggesting a shift towards increasing aragonite deposition since the Eocene. A major criticism of the hypothesis for a mineralogical control on the  $\delta^{44/40}\text{Ca}_{\text{sw}}$  is that it assumes that the Ca isotopic composition of the primary carbonate minerals are preserved during diagenetic stabilization and sediment burial. In contrast, recent studies of  $\delta^{44/40}\text{Ca}$  values and major/minor elements in Neogene neritic sediments from the Bahamas (Higgins et al., 2018) and Australia (Fantle and Higgins, 2014) indicate that 'typical' diagenetic conditions in these environments can increase bulk sediment  $\delta^{44/40}\text{Ca}$  values by  $>1\%$  and lower Sr contents by  $>90\%$  compared to unaltered primary carbonate sediment. If these results are representative of the global neritic carbonate sink, they suggest that the primary mineralogy (e.g. aragonite or calcite) plays only a minor role in determining the average  $\delta^{44/40}\text{Ca}$  value and Sr content of neritic carbonate sediments. Rather, the average  $\delta^{44/40}\text{Ca}$  value and Sr content of the neritic carbonate sink appears to depend largely on the extent and style of diagenetic alteration.

#### 4.4.2. The Mid-Mesozoic revolution in pelagic calcification - implications for the chemical and isotopic composition of seawater

The evolution of planktonic calcifiers and their radiation in the mid-Mesozoic had profound consequences for the production and burial of carbonate minerals in the ocean (Ridgwell, 2005). While it is recognized that these changes produced a shift in the locus of carbonate burial in the ocean from neritic to pelagic environments, resulting in a suite of feedbacks that stabilize carbonate saturation in the ocean ('carbonate compensation'; Ridgwell, 2005), the effects of the accompanying decline in the neritic carbonate sink are less well understood. As the average  $\delta^{44/40}\text{Ca}$  value and Sr content of the neritic carbonate sink depends more on diagenesis than primary mineralogy (Section 4.4.1), we propose that the decline in the

**Table 2**

Summary of model notation and values for preferred model output (Fig. 8A).

Notation	Definition	Value
$K_{\text{neritic}}^{\text{Sr/Ca}}$	Sr partitioning coefficient; neritic carbonates	0.134 <sup>a</sup>
$K_{\text{pelagic}}^{\text{Sr/Ca}}$	Sr partitioning coefficient; pelagic carbonates	0.035 <sup>b</sup>
$\delta^{44}\text{Ca}_{\text{input}}$	isotopic composition of inputs (‰)	-1.1
$\epsilon_{\text{pelagic}}^{\text{Ca}}$	fractionation factor for pelagic carbonates	variable; see text
$\epsilon_{\text{neritic}}^{\text{Ca}}$	fractionation factor for neritic carbonates	0.5
$f$	fraction of neritic carbonate sedimentation	variable, see text <sup>c</sup>

<sup>a</sup> From average neritic carbonate Sr/Ca = 1.15 mmol/mol (Fantle and Higgins, 2014; Higgins et al., 2018).

<sup>b</sup> From average pelagic carbonate Sr/Ca = 0.3 mmol/mol.

<sup>c</sup> Adapted from Opdyke and Wilkinson (1988) and shown in Fig. 8D.

neritic carbonate sink due to the growth of the pelagic carbonate sink and declining tropical shelf area provides an alternative mechanism to explain the increase in  $\delta^{44/40}\text{Ca}_{\text{sw}}$  and decline in  $[\text{Sr}]_{\text{sw}}$  over the last 100 million years.

We quantitatively model these changes using equations (3a)–(3b), accounting for the size of the neritic and pelagic carbonate sinks, the fractionation ( $\epsilon$ ) associated with each reservoir, and the Sr partitioning coefficient ( $K_{\text{neritic}}^{\text{Sr/Ca}}$ ) for the neritic sink. Results of the preferred-fit model using the variables are listed in Table 2 and shown in Figs. 6C and 8. We estimate Ca isotope fractionation ( $\epsilon_{\text{neritic}}^{\text{Ca}} = 0.5\%$ ) and Sr partitioning ( $K_{\text{neritic}}^{\text{Sr/Ca}} = 0.134$ , from an average neritic concentration of 1.15 mmol/mol) in the neritic carbonate sink empirically using measurements of Neogene neritic limestones and dolomites from the Bahamas and Australia (Fantle and Higgins, 2014; Higgins et al., 2018) and assuming the diagenetic fluid is unaltered seawater ( $\delta^{44/40}\text{Ca} = 0\%$ ; Sr/Ca = 8.6 mmol/mol). The values of  $\epsilon_{\text{neritic}}^{\text{Ca}}$  and  $K_{\text{neritic}}^{\text{Sr/Ca}}$  approach estimates for equilibrium fractionation of Ca isotopes in calcite (Fantle and DePaolo, 2007) and the partitioning of Sr into stoichiometric secondary dolomite (Vahrenkamp and Swart, 1990). This assumption is akin to saying that the neritic carbonate sink is partially equilibrated with seawater during early marine diagenesis. Importantly, these values result in a neritic carbonate sink that is almost 1‰ higher in its  $\delta^{44/40}\text{Ca}$  value ( $-0.5\%$  compared to  $-1.3\%$ ) and a factor of 4 lower in its Sr/Ca ratio ( $\sim 0.3$  compared to 1.15 mmol/mol) than the modern pelagic carbonate sink (Fantle and Higgins, 2014; Ahm et al., 2018; Higgins et al., 2018). The value for  $\epsilon_{\text{pelagic}}^{\text{Ca}}$  is determined from the difference between the  $\delta^{44/40}\text{Ca}_{\text{sw}}$  and  $\delta^{44/40}\text{Ca}_{\text{pelagic}}$ , where the former is inferred from our fossil elasmobranch record and the latter from measurements of bulk pelagic carbonate over the Cenozoic (Fantle and DePaolo, 2005, 2007; Gothmann et al., 2016). Using this approach, we calculate an increase in  $\epsilon_{\text{pelagic}}^{\text{Ca}}$  from 0.8‰ in the late Mesozoic to approximately 1.25‰ today (Fig. 8C). The origins of this change are enigmatic at present, but likely reflect a combination of factors including changes in vital effects associated with biomineralization (Gothmann et al., 2016; Gussone et al., 2016) and changes in taxonomic assemblages (Martin, 1995).

Figs. 8 and 6C show that a simple model of the global Ca and Sr cycles that includes both the effects of a declining neritic carbonate sink and changes in Ca isotope fractionation associated with the pelagic carbonate sink, quantitatively reproduces both the increase in seawater  $\delta^{44/40}\text{Ca}$  values and the decline in seawater Sr concentrations over the last 100 million years. Although this model solution is not unique, it is grounded in robust independent observations of changes in the partitioning of the global carbonate sink between neritic and pelagic environments and our understanding of how the chemical and isotopic composition of these sinks are altered by diagenetic recrystallization and neomorphism. In addition, our model makes predictions for the seawater Ca isotopic composition of the pre-Mesozoic ocean as prior to the proliferation of pelagic calcifying organisms the global carbonate sink is under-

stood to be exclusively neritic. Assuming an  $\varepsilon_{\text{neritic}}^{\text{Ca}}$  of 0.5‰ (see discussion above), the predicted  $\delta^{44/40}\text{Ca}$  value for seawater is approximately  $-0.6\text{‰}$ , broadly in agreement with published records of Phanerozoic seawater (Farkaš et al., 2007; Blättler et al., 2012).

Although beyond the scope of this manuscript, the secular change in the flux of Sr associated with diagenetic recrystallization of shallow-water carbonate sediments should also have an effect on the  $^{87}\text{Sr}/^{86}\text{Sr}$  mass balance of seawater. Rapid recycling of Sr between seawater and shallow-water carbonate sediments provides inertia to seawater  $^{87}\text{Sr}/^{86}\text{Sr}$  ratios by effectively increasing the size of the seawater Sr reservoir: when rates of shallow-water carbonate recrystallization are high, larger changes in the flux and/or isotopic composition of continental weathering or hydrothermal sources of Sr are needed to change seawater  $^{87}\text{Sr}/^{86}\text{Sr}$ . Conversely, when recrystallization rates are low, seawater  $^{87}\text{Sr}/^{86}\text{Sr}$  ratios will be more sensitive to changes in the magnitude and/or isotopic composition of Sr sources from continental weathering and/or mid-ocean ridge hydrothermal systems.

## 5. Conclusions

- Elasmobranch tooth enamel can be used as an archive of seawater chemistry. Although taxonomical variability and ontogenetic history of individual taxa likely contribute to the range in recorded  $\delta^{44/40}\text{Ca}$  and Sr/Ca in modern specimens, large and diverse sample sets can capture the full range of variability and provide robust reconstructions of paleoseawater chemistry.
- Elasmobranch tooth enamel record an increase in seawater  $\delta^{44/40}\text{Ca}$  values over the last 100 million years, in agreement with independent archives including well-preserved corals and bulk carbonates. We attribute the increase in the  $\delta^{44/40}\text{Ca}$  of seawater to changes in the Ca isotopic composition of the global marine carbonate sink. In particular, the increase in seawater  $\delta^{44/40}\text{Ca}$  values is best explained as the consequence of an expansion of the pelagic carbonate sink at the expense of shallow carbonate platforms. The decline in shallow-water carbonate sediments reduces the diagenetic flux of Ca with low  $\delta^{44/40}\text{Ca}$  values, leading to an increase in the  $\delta^{44/40}\text{Ca}$  value of seawater since the Mesozoic.
- A decline in shallow-water carbonate sediments associated with the expansion of pelagic calcifiers in the Mid-Mesozoic also provides an explanation for the four-fold decline in  $[\text{Sr}]_{\text{sw}}$  over the same time period. This result highlights the important role that early marine diagenesis in the global geochemical cycles of Ca and Sr.

## Declaration of competing interest

The authors declare that they have no known competing financial interests or personal relationships that could have appeared to influence the work reported in this paper.

## Acknowledgements

We thank Dr. Ted Daeschler (Academy of Natural Sciences of Drexel University), Dr. Hans-Dieter Sues (Smithsonian Institution), Bruce Schumacher (USDA Forest Service), Dr. Christian Shorey (Colorado School of Mines), Robert Kirkham (Geological Solutions, Inc.), Dr. Dewayne Fox (Delaware State University), Dr. Kate Siegfried (NOAA National Marine Fisheries Service), and Calvert Marine Museum for loaning samples. Liz Lundstrom and Nic Slater provided laboratory assistance. Emma Kast, Yuzhen Yan, Michael Bender and Danny Sigman provided helpful discussion and feedback. We would like to thank 2 anonymous reviewers and Lou Derry for

constructive comments that improved this manuscript. AAA acknowledges support from the Scott Vertebrate Paleontology Fund (Princeton University). This research was supported in part by National Science Foundation Sedimentary Geology and Paleobiology Award to Michael Griffiths, Robert Eagle and Martin Becker (1830581) and Sora Kim (1830480), and American Chemical Society Award Petroleum Research Fund Undergraduate New Investigator Grant, PRF-#54852-UNI2, to MLG.

## Appendix A. Supplementary material

Supplementary material related to this article can be found online at <https://doi.org/10.1016/j.epsl.2020.116354>.

## References

- Ahm, A.-S.C., Bjerrum, C.J., Blättler, C.L., Swart, P.K., Higgins, J.A., 2018. Quantifying early marine diagenesis in shallow-water carbonate sediments. *Geochim. Cosmochim. Acta* 236, 140–159. <https://doi.org/10.1016/j.gca.2018.02.042>.
- Balter, V., Lécuyer, C., 2004. Determination of Sr and Ba partition coefficients between apatite and water from 5°C to 60°C: a potential new thermometer for aquatic paleoenvironments. *Geochim. Cosmochim. Acta* 68, 423–432. [https://doi.org/10.1016/S0016-7037\(00\)00453-8](https://doi.org/10.1016/S0016-7037(00)00453-8).
- Balter, V., Lécuyer, C., Barrat, J.A., 2011. Reconstructing seawater Sr/Ca during the last 70 My using fossil fish tooth enamel. *Palaeogeogr. Palaeoclimatol. Palaeoecol.* 310, 133–138. <https://doi.org/10.1016/j.palaeo.2011.02.024>.
- Blättler, C.L., Henderson, G.M., Jenkyns, H.C., 2012. Explaining the Phanerozoic Ca isotope history of seawater. *Geology* 40, 843–846. <https://doi.org/10.1130/G33191.1>.
- Blättler, C.L., Higgins, J.A., 2017. Testing Urey's carbonate-silicate cycle using the calcium isotopic composition of sedimentary carbonates. *Earth Planet. Sci. Lett.* 479, 241–251. <https://doi.org/10.1016/j.epsl.2017.09.033>.
- Boyle, E.A., Keigwin, L.D., 1985. Comparison of Atlantic and Pacific paleochemical records for the last 215,000 years: changes in deep ocean circulation and chemical inventories. *Earth Planet. Sci. Lett.* 76, 135–150.
- Clementz, M.T., Holden, P., Koch, P.L., 2003. Are calcium isotopes a reliable monitor of trophic level in marine settings? *Int. J. Osteoarchaeol.* 13, 29–36. <https://doi.org/10.1002/oa.657>.
- Coggon, R.M., Teagle, D.A.H., Smith-Duque, C.E., Alt, J.C., Cooper, M.J., 2010. Reconstructing past seawater Mg/Ca and Sr/Ca from mid-ocean ridge flank calcium carbonate veins. *Science* 327, 1114–1117. <https://doi.org/10.1126/science.1182252>.
- Coogan, L.A., 2009. Altered oceanic crust as an inorganic record of paleoseawater Sr concentration. *Geochem. Geophys. Geosyst.* 10. <https://doi.org/10.1029/2008GC002341>.
- DePaolo, D.J., 2011. Surface kinetic model for isotopic and trace element fractionation during precipitation of calcite from aqueous solutions. *Geochim. Cosmochim. Acta* 75, 1039–1056. <https://doi.org/10.1016/j.gca.2010.11.020>.
- Elderfield, H., Schultz, A., 1996. Mid-ocean ridge hydrothermal fluxes and the chemical composition of the ocean. *Annu. Rev. Earth Planet. Sci.* 24, 191–224.
- Fantle, M.S., DePaolo, D.J., 2005. Variations in the marine Ca cycle over the past 20 million years. *Earth Planet. Sci. Lett.* 237, 102–117.
- Fantle, M.S., DePaolo, D.J., 2006. Sr isotopes and pore fluid chemistry in carbonate sediment of the Ontong Java Plateau: calcite recrystallization rates and evidence for a rapid rise in seawater Mg over the last 10 million years. *Geochim. Cosmochim. Acta* 70, 3883–3904.
- Fantle, M.S., DePaolo, D.J., 2007. Ca isotopes in carbonate sediment and pore fluid from ODP site 807A: the Ca<sub>2</sub>+(aq)-calcite equilibrium fractionation factor and calcite recrystallization rates in Pleistocene sediments. *Geochim. Cosmochim. Acta* 71, 2524–2546.
- Fantle, M.S., Higgins, J., 2014. The effects of diagenesis and dolomitization on Ca and Mg isotopes in marine platform carbonates: implications for the geochemical cycles of Ca and Mg. *Geochim. Cosmochim. Acta* 142, 458–481. <https://doi.org/10.1016/j.gca.2014.07.025>.
- Fantle, M.S., Tipper, E.T., 2014. Calcium isotopes in the global biogeochemical Ca cycle: implications for development of a Ca isotope proxy. *Earth-Sci. Rev.* 129. <https://doi.org/10.1016/j.earscirev.2013.10.004>.
- Farkaš, J., Böhm, F., Wallmann, K., Blenkinsop, J., Eisenhauer, A., van Geldern, R., Munnecke, A., Voigt, S., Veizer, J., 2007. Calcium isotope record of Phanerozoic oceans: implications for chemical evolution of seawater and its causative mechanisms. *Geochim. Cosmochim. Acta* 71, 5117–5134.
- Fischer, J., Voigt, S., Franz, M., Schneider, J.W., Joachimski, M.M., Tichomirowa, M., Götze, J., Furrer, H., 2012. Palaeoenvironments of the late Triassic Rhaetian Sea: implications from oxygen and strontium isotopes of hybodont shark teeth. *Palaeogeogr. Palaeoclimatol. Palaeoecol.* 353–355, 60–72. <https://doi.org/10.1016/j.palaeo.2012.07.002>.

- Froese, R., Pauly, D., 2019. FishBase. Available at [www.fishbase.org](http://www.fishbase.org).
- Gothmann, A.M., Bender, M.L., Blättler, C.L., Swart, P.K., Giri, S.J., Adkins, J.F., Stolarzki, J., Higgins, J.A., 2016. Calcium isotopes in scleractinian fossil corals since the Mesozoic: implications for vital effects and biomineralization through time. *Earth Planet. Sci. Lett.* 444, 205–214. <https://doi.org/10.1016/j.epsl.2016.03.012>.
- Gothmann, A.M., Stolarzki, J., Adkins, J.F., Schoene, B., Dennis, K.J., Schrag, D.P., Mazur, M., Bender, M.L., 2015. Fossil corals as an archive of secular variations in seawater chemistry since the Mesozoic. *Geochim. Cosmochim. Acta* 160, 188–208. <https://doi.org/10.1016/j.gca.2015.03.018>.
- Griffith, E.M., Paytan, A., Caldeira, K., Bullen, T., Thomas, E., 2008. A dynamic marine calcium cycle during the past 28 million years. *Science* 322, 1671–1674. Available at <http://science.sciencemag.org/content/322/5908/1671>.
- Griffiths, N., Müller, W., Johnson, K.G., Aguilera, O.A., 2013. Evaluation of the effect of diagenetic cements on element/Ca ratios in aragonitic Early Miocene (~16 Ma) Caribbean corals: implications for “deep-time” palaeo-environmental reconstructions. *Palaeogeogr. Palaeoclimatol. Palaeoecol.* 369, 185–200.
- Gussone, N., Böhm, F., Eisenhauer, A., Dietzel, M., Heuser, A., Teichert, B.M.A., Reitner, J., Wörheide, G., Dullo, W.C., 2005. Calcium isotope fractionation in calcite and aragonite. *Geochim. Cosmochim. Acta* 69, 4485–4494.
- Gussone, N., Filipsson, H.L., Kuhnert, H., 2016. Mg/Ca, Sr/Ca and Ca isotope ratios in benthonic foraminifers related to test structure, mineralogy and environmental controls. *Geochim. Cosmochim. Acta* 173, 142–159. <https://doi.org/10.1016/j.gca.2015.10.018>.
- Hardie, L.A., 1996. Secular variation in seawater chemistry: an explanation for the coupled secular variation in the mineralogies of marine limestones and potash evaporites over the past 600 m.y. *Geology* 24, 279–283.
- Heuser, A., Eisenhauer, A., 2008. The calcium isotope composition ( $\delta^{44}/^{40}\text{Ca}$ ) of NIST SRM 915b and NIST SRM 1486. *Geostand. Geoanal. Res.* 32, 311–315.
- Heuser, A., Eisenhauer, A., 2010. A pilot study on the use of natural calcium isotope ( $^{44}\text{Ca}/^{40}\text{Ca}$ ) fractionation in urine as a proxy for the human body calcium balance. *Bone* 46, 889–896. <https://doi.org/10.1016/j.bone.2009.11.037>.
- Heuser, A., Eisenhauer, A., Bo, F., Wallmann, K., Gussone, N., Pearson, P.N., Na, T.F., 2005. Calcium isotope ( $\text{D } 44 / 40 \text{ Ca}$ ) variations of Neogene planktonic foraminifera. *Paleoceanography* 20, 1–13.
- Higgins, J.A., Blättler, C.L., Lundstrom, E.A., Santiago-Ramos, D.P., Akhtar, A.A., Crüger Ahm, A.-S., Bialik, O., Holmden, C., Bradbury, H., Murray, S.T., Swart, P.K., 2018. Mineralogy, early marine diagenesis, and the chemistry of shallow-water carbonate sediments. *Geochim. Cosmochim. Acta* 220, 512–534. Available at <http://linkinghub.elsevier.com/retrieve/pii/S001670371730635X>.
- Horita, J., Zimmermann, H., Holland, H.D., 2002. Chemical evolution of seawater during the Phanerozoic. *Geochim. Cosmochim. Acta* 66, 3733–3756.
- Ivany, L.C., Peters, S., Wilkinson, B.H., Lohmann, K.C., Reimer, B.A., 2004. Composition of the early Oligocene ocean from coral stable isotope and elemental chemistry. *Geobiology* 2, 97–106. <https://doi.org/10.1111/j.1472-4677.2004.00025.x>.
- Jacobson, A.D., Grace Andrews, M., Lehn, G.O., Holmden, C., 2015. Silicate versus carbonate weathering in Iceland: new insights from Ca isotopes. *Earth Planet. Sci. Lett.* 416, 132–142. <https://doi.org/10.1016/j.epsl.2015.01.030>.
- Kocsis, L., Vennemann, T.W., Hegner, E., Fontignie, D., Tütken, T., 2009. Constraints on Miocene oceanography and climate in the Western and Central Paratethys: O-, Sr-, and Nd-isotope compositions of marine fish and mammal remains. *Palaeogeogr. Palaeoclimatol. Palaeoecol.* 271, 117–129. <https://doi.org/10.1016/j.palaeo.2008.10.003>.
- Kocsis, L., Vennemann, T.W., Ulianov, A., Brunnschweiler, J.M., 2015. Characterizing the bull shark *Carcharhinus leucas* habitat in Fiji by the chemical and isotopic compositions of their teeth. *Environ. Biol. Fishes* 98, 1609–1622.
- Lear, C.H., Elderfield, H., Wilson, P.A., 2003. A Cenozoic seawater Sr/Ca record from benthic foraminiferal calcite and its application in determining global weathering fluxes. *Earth Planet. Sci. Lett.* 208, 69–84. [https://doi.org/10.1016/S0012-821X\(02\)01156-1](https://doi.org/10.1016/S0012-821X(02)01156-1).
- Lowenstein, T.K., Hardie, L.A., Timofeeff, M.N., Demicco, R.V., 2003. Secular variation in seawater chemistry and the origin and significance of calcium chloride brines. In: *Geol. Soc. Am. 2003 Annu. Meet. Seattle, WA, United States, Nov. 2-5, vol. 35. Geological Society of America, p. 201. 2003 annual meeting.*
- Martin, J.E., Tacail, T., Adnet, S., Girard, C., Balter, V., 2015. Calcium isotopes reveal the trophic position of extant and fossil elasmobranchs. *Chem. Geol.* 415, 118–125. <https://doi.org/10.1016/j.chemgeo.2015.09.011>.
- Martin, R.E., 1995. Cyclic and secular variation in microfossil biomineralization: clues to the biogeochemical evolution of Phanerozoic oceans. *Glob. Planet. Change* 11, 1–23.
- McArthur, J.M., Howarth, R.J., Bailey, T.R., 2001. Strontium isotope stratigraphy: LOWESS version 3: best fit to the marine Sr-isotope curve for 0–509 Ma and accompanying look-up table for deriving numerical age. *J. Geol.* 109, 155–170. <https://doi.org/10.1086/319243>. Available at <http://discovery.ucl.ac.uk/8838/>. <http://eprints.ucl.ac.uk/8838/>.
- McArthur, J.M., Kennedy, W.J., Chen, M., Thirlwall, M.F., Gale, A.S., 1994. Strontium isotope stratigraphy for Late Cretaceous time: direct numerical calibration of the Sr isotope curve based on the US Western Interior. *Palaeogeogr. Palaeoclimatol. Palaeoecol.* 108, 95–119.
- Melim, L.A., Westphal, H., Swart, P.K., Eberli, G.P., Munnecke, A., 2002. Questioning carbonate diagenetic paradigms: evidence from the Neogene of the Bahamas. *Mar. Geol.* 185, 27–53.
- Morgan, J.L.L., Skulan, J.L., Gordon, G.W., Romaniello, S.J., Smith, S.M., Anbar, A.D., 2012. Rapidly assessing changes in bone mineral balance using natural stable calcium isotopes. *Proc. Natl. Acad. Sci. USA* 109, 9989–9994.
- Nielsen, L.C., De Yoreo, J.J., DePaolo, D.J., 2013. General model for calcite growth kinetics in the presence of impurity ions. *Geochim. Cosmochim. Acta* 115, 100–114. <https://doi.org/10.1016/j.gca.2013.04.001>.
- Opydyke, B.N., Wilkinson, B.H., 1988. Surface area control of shallow cratonic to deep marine carbonate accumulation. *Paleoceanography* 3, 685–703.
- Rausch, S., Böhm, F., Bach, W., Klügel, A., Eisenhauer, A., 2013. Calcium carbonate veins in ocean crust record a threefold increase of seawater Mg/Ca in the past 30 million years. *Earth Planet. Sci. Lett.* 362, 215–224.
- Reynard, B., Lécuyer, C., Grandjean, P., 1999. Crystal-chemical controls on rare-earth element concentrations in fossil biogenic apatites and implications for paleoenvironmental reconstructions. *Chem. Geol.* 155, 233–241.
- Richter, F.M., DePaolo, D.J., 1987. Numerical models for diagenesis and the Neogene Sr isotopic evolution of seawater from DSDP Site 590B. *Earth Planet. Sci. Lett.* 83, 27–38.
- Ridgwell, A., 2005. A Mid Mesozoic Revolution in the regulation of ocean chemistry. *Mar. Geol.* 217, 339–357. <https://doi.org/10.1016/j.margeo.2004.10.036>.
- Rosenthal, Y., Field, M.P., Sherrell, R.M., 1999. Precise determination of element/calcium ratios in calcareous samples using sector field inductively coupled plasma mass spectrometry. *Anal. Chem.* 71, 3248–3253.
- Sandberg, P.A., 1983. An oscillating trend in Phanerozoic non-skeletal carbonate mineralogy. *Nature* 305, 19–22.
- Sime, N.G., De La Rocha, C.L., Tipper, E.T., Tripathi, A., Galy, A., Bickle, M.J., 2007. Interpreting the Ca isotope record of marine biogenic carbonates. *Geochim. Cosmochim. Acta* 71, 3979–3989.
- Skulan, J., DePaolo, D.J., 1999. Calcium isotope fractionation between soft and mineralized tissues as a monitor of calcium use in vertebrates. *Proc. Natl. Acad. Sci. USA* 96, 13709–13713.
- Sosdian, S.M., Lear, C.H., Tao, K., Grossman, E.L., O’Dea, A., Rosenthal, Y., 2012. Cenozoic seawater Sr/Ca evolution. *Geochem. Geophys. Geosyst.* 13, 1–23.
- Soudry, D., Glenn, C.R., Nathan, Y., Segal, I., Vonderhaar, D., 2006. Evolution of Tethyan phosphogenesis along the northern edges of the Arabian – African shield during the Cretaceous – Eocene as deduced from temporal variations of Ca and Nd isotopes and rates of P accumulation. *Earth-Sci. Rev.* 78, 27–57.
- Soudry, D., Segal, I., Nathan, Y., Glenn, C.R., Halicz, L., Lewy, Z., Vonderhaar, D.L., 2004.  $^{44}\text{Ca}/^{42}\text{Ca}$  and  $^{143}\text{Nd}/^{144}\text{Nd}$  isotope variations in Cretaceous – Eocene Tethyan francolites and their bearing on phosphogenesis in the southern Tethys. *Geology* 32, 389–392. <https://doi.org/10.1130/G20438.1>.
- Steuber, T., Veizer, J., 2002. Phanerozoic record of plate tectonic control of seawater chemistry and carbonate sedimentation. *Geology* 30, 1123–1126.
- Stoll, H.M., Schrag, D.P., 1998. Effects of Quaternary sea level cycles on Sr in seawater. *Geochim. Cosmochim. Acta* 62, 1107–1118. Available at <http://www.sciencedirect.com/science/article/pii/S0016703798000428>.
- Sundell, K., Björnsson, B.T., 1988. Kinetics of calcium fluxes across the Intestinal Mucosa of the Marine Teleost, *Gadus Morhua*, measured using an in vitro perfusion method. *J. Exp. Biol.* 140, 171–186.
- Swart, P.K., Eberli, G., 2005. The nature of the  $\delta^{13}\text{C}$  of periplatform sediments: implications for stratigraphy and the global carbon cycle. *Sediment. Geol.* 175, 115–129.
- Swart, P.K., Melim, L.A., 2000. The origin of dolomites in tertiary sediments from the margin of Great Bahama Bank. *J. Sediment. Res.* 70 (2).
- Swart, P.K., Melim, L.A., 2003. The origin of dolomites in tertiary sediments from the margin of Great Bahama Bank. *J. Sediment. Res.* 70, 738–748. <https://doi.org/10.1306/d4268c98-2b26-11d7-8648000102c1865d>.
- Tacail, T., Albalat, E., Télouk, P., Balter, V., 2014. A simplified protocol for measurement of Ca isotopes in biological samples. *J. Anal. At. Spectrom.* 29, 529. Available at <http://xlink.rsc.org/?DOI=c3ja50337b>.
- Tang, J., Dietzel, M., Böhm, F., Köhler, S.J., Eisenhauer, A., 2008.  $\text{Sr}^{2+}/\text{Ca}^{2+}$  and  $^{44}\text{Ca}/^{40}\text{Ca}$  fractionation during inorganic calcite formation: II. Ca isotopes. *Geochim. Cosmochim. Acta* 72, 3733–3745.
- Tripathi, A.K., Allmon, W.D., Sampson, D.E., 2009. Possible evidence for a large decrease in seawater strontium/calcium ratios and strontium concentrations during the Cenozoic. *Earth Planet. Sci. Lett.* 282, 122–130. <https://doi.org/10.1016/j.epsl.2009.03.020>.
- Vahrenkamp, V.C., Swart, P.K., 1990. New distribution coefficient for the incorporation of strontium into dolomite and its implications for the formation of ancient dolomites. *Geology* 18, 387–391.
- van der Ploeg, R., Boudreau, B.P., Middelburg, J.J., Sluijs, A., 2019. Cenozoic carbonate burial along continental margins. *Geology* 47.
- Walker, L.J., Wilkinson, B.H., Ivany, L.C., 2002. Continental drift and Phanerozoic carbonate accumulation in shallow-shelf and deep-marine settings. *J. Geol.* 110, 75–87. Available at <http://www.journals.uchicago.edu/doi/10.1086/324318>.
- Wilga, C.D., Motta, P.J., Sanford, C.P., 2007. Evolution and ecology of feeding in elasmobranchs. *Integr. Comp. Biol.* 47, 55–69.

Zeichner, S.S., Colman, A.S., Koch, P.L., Polo-Silva, C., Galván-Magaña, F., Kim, S.L., 2017. Discrimination factors and incorporation rates for organic matrix in shark teeth based on a captive feeding study. *Physiol. Biochem. Zool.* 90, 257–272.

Zhu, P., Douglas Macdougall, J., 1998. Calcium isotopes in the marine environment and the oceanic calcium cycle. *Geochim. Cosmochim. Acta* 62, 1691–1698. [https://doi.org/10.1016/S0016-7037\(98\)00110-0](https://doi.org/10.1016/S0016-7037(98)00110-0).